

# THE ACCRETION DISK LIMIT CYCLE MECHANISM IN THE BLACK HOLE X-RAY BINARIES: TOWARD AN UNDERSTANDING OF THE SYSTEMATIC EFFECTS

JOHN K. CANNIZZO<sup>1</sup>

NASA/Goddard Space Flight Center, Laboratory for High Energy Astrophysics, Code 662, Greenbelt, MD 20771;  
 cannizzo@lheavx.gsfc.nasa.gov

Received 1997 July 21; accepted 1997 September 17

## ABSTRACT

We examine in detail several aspects of the physics of accretion disks that are of possible relevance to the outburst mechanism of the black hole X-ray transients. We adopt the one-dimensional, time-dependent model described in detail by Cannizzo, Chen, and Livio with parameters appropriate for a system such as A0620–00. We investigate (1) the effect of the grid spacing, utilizing a logarithmic radial spacing  $\Delta r \propto r$  in addition to the spacing  $\Delta r \propto r^{1/2}$ , (2) the dependence of the local flow speed of gas within the hot part of the disk on radius and time during the time of the cooling wave propagation, (3) the shape of the outburst light curve as a function of the triggering location for the instability, (4) the long-term light curves of outbursts taken from trials in which complete cycles of quiescence and outburst are followed, both including and excluding the effect of evaporation or removal of matter from the inner edge of the disk, and (5) the strength of the self-irradiation of the outer parts of the disk by the X-rays from the inner disk. Our primary findings in each of these areas are that (1) low-resolution runs taking  $N \simeq 20$  grid points using the logarithmic spacing produce decay timescales that are artificially slow by factors of  $\sim 2$ – $3$  and slower than exponential; (2) the deviation from steady state within the outer part of the inner hot disk appears to be in accord with the discussion given in Vishniac and Wheeler—far from the transition front, the flow speed is  $\sim \alpha c_s(h/r)$ , whereas at the interface between the transition front and the cold disk, the flow speed is  $\sim \alpha c_s$ ; (3) the outburst-triggering location must be  $\gtrsim 100r_{\text{inner}}$  for the rise time of the resulting outburst to be as short as is observed in the standard, bright systems; (4) the long-term light curves using the standard model produce frequent outbursts that are triggered near the inner disk edge and that have slow rise times, and the long-term light curves calculated assuming evaporation of matter from the inner disk exhibit outbursts with longer recurrence times and somewhat (but not significantly) shorter rise times; and (5) for a system with parameters relevant to A0620–00, our “standard” system, irradiation is not a dynamically significant effect, in accord with recent results of van Paradijs.

*Subject headings:* accretion, accretion disks — binaries: close — black hole physics — stars: individual (A0620–00) — X-rays: bursts — X-rays: stars

## 1. INTRODUCTION

The black hole X-ray binaries (BHXBs) are interacting binary systems in which a Roche lobe–filling K- or M-type secondary transfers matter through the inner Lagrangian point into orbit around a black hole accretor. The systems are therefore similar in many respects to the cataclysmic variables, the difference being that the accretor is not a white dwarf (for a critical comparison of soft X-ray transients and dwarf novae, see van Paradijs & Verbunt 1984). The BHXBs were discovered because of large outbursts seen first in X-rays that lasted weeks to months. The systems were subsequently studied optically and found to be binary systems with orbital periods of several hours to several days, and with large mass functions,  $f(M) \gtrsim 3 M_{\odot}$ , that imply black hole primaries (van Paradijs & McClintock 1995).

The accretion disk limit cycle mechanism that was originally put forth to account for the dwarf nova outbursts (Meyer & Meyer-Hofmeister 1981; for recent reviews see Cannizzo 1993a, 1998b; Osaki 1996) should work in other interacting binary stars. The model basically operates because of an inherent hysteretic relation between the vertically integrated viscous stress,  $\nu\Sigma$ , and the surface density,  $\Sigma$ , at a fixed radius in the disk. The quantity  $\nu$  is the kinematic viscosity coefficient,  $\nu = 2\alpha P/(3\Omega\rho)$ , and  $\alpha$  is the Shakura & Sunyaev (1973) parameter characterizing the magnitude of the viscous stress. When equilibrium solutions are plotted as  $\log \nu\Sigma$  (or  $\log T_{\text{effective}}$ ) versus  $\log \Sigma$ , one sees an S-curve relation. The lower and upper branches of the S that have positive slope are thermally and viscously stable, whereas the middle, negatively sloping portion of the S is unstable. During quiescence, the gas in the accretion disk is far from steady state: matter accumulates at large radii in the disk, and almost none reaches the central object. The gas is neutral, and the temperature and surface density values it possesses place it along the lower, stable portion of the S-curve. As matter continues to pile up, at some point a critical surface density,  $\Sigma_{\text{max}}$ , corresponding to the local maximum in the S-curve, is exceeded, and a heating instability is initiated that ultimately takes all or most of the disk to the hot state wherein the gas is ionized and resides along the upper stable branch of the S-curve. The rate of viscous evolution is much greater than before, and the  $\Sigma(r)$  profile shifts to a near steady state configuration in which  $\Sigma(r)$  decreases with radius, in contrast to the quiescent configuration in which  $\Sigma(r)$  increases with radius. After some material has accreted onto the central object and produced an outburst, the surface density decreases until at some point the local value drops below another critical value,  $\Sigma_{\text{min}}$ , that characterizes the lower bend in the S-curve. This always happens near the outer disk edge and initiates a

matic viscosity coefficient,  $\nu = 2\alpha P/(3\Omega\rho)$ , and  $\alpha$  is the Shakura & Sunyaev (1973) parameter characterizing the magnitude of the viscous stress. When equilibrium solutions are plotted as  $\log \nu\Sigma$  (or  $\log T_{\text{effective}}$ ) versus  $\log \Sigma$ , one sees an S-curve relation. The lower and upper branches of the S that have positive slope are thermally and viscously stable, whereas the middle, negatively sloping portion of the S is unstable. During quiescence, the gas in the accretion disk is far from steady state: matter accumulates at large radii in the disk, and almost none reaches the central object. The gas is neutral, and the temperature and surface density values it possesses place it along the lower, stable portion of the S-curve. As matter continues to pile up, at some point a critical surface density,  $\Sigma_{\text{max}}$ , corresponding to the local maximum in the S-curve, is exceeded, and a heating instability is initiated that ultimately takes all or most of the disk to the hot state wherein the gas is ionized and resides along the upper stable branch of the S-curve. The rate of viscous evolution is much greater than before, and the  $\Sigma(r)$  profile shifts to a near steady state configuration in which  $\Sigma(r)$  decreases with radius, in contrast to the quiescent configuration in which  $\Sigma(r)$  increases with radius. After some material has accreted onto the central object and produced an outburst, the surface density decreases until at some point the local value drops below another critical value,  $\Sigma_{\text{min}}$ , that characterizes the lower bend in the S-curve. This always happens near the outer disk edge and initiates a

<sup>1</sup> Universities Space Research Association.

cooling wave that propagates inward to smaller radii, shutting off the flow and reverting the disk material back into neutral gas. If this model is correct, one cannot avoid having the limit cycle instability operating—unless the mass transfer rate feeding into the outer edge exceeds a critical value (Smak 1983) or irradiation is able to keep the entire disk permanently ionized (Tuchman, Mineshige, & Wheeler 1990; van Paradijs 1996). Not long after its introduction, various workers began to apply the model to the soft X-ray transients, a class that includes systems with both neutron star and black hole accretors (Cannizzo, Wheeler, & Ghosh 1982, 1985; Lin & Taam 1984; Huang & Wheeler 1989, hereafter HW; Mineshige & Wheeler 1989, hereafter MW).

Cannizzo, Chen, & Livio (1995; hereafter, CCL) investigated in detail the decay of the light curves accompanying the outbursts in the BHXBs. They discovered that, if a cooling wave is responsible for the decay of the outbursts, then the observed exponential decay of the soft X-ray fluxes in the BHXBs constrains the viscosity parameter,  $\alpha$ , to have the form  $\alpha = \alpha_0(h/r)^{1.5}$ , where  $\alpha_0 \approx 50$  if the primary (i.e., black hole) mass in the BHXBs is  $\sim 10 M_\odot$ . This form was introduced by Meyer & Meyer-Hofmeister (1983, 1984). The value of  $\sim 50$  for the proportionality constant is mandated by the observed  $\sim 30$  day  $e$ -folding decay times for outbursts in the BHXBs. The constraint is actually on  $M_1/\alpha_0$ . A recent compilation of inferred black hole masses for BHXBs by Bailyn et al. (1996) seems to indicate that the distribution is strongly peaked at  $\sim 7 M_\odot$ , whereas the value  $\alpha_0 \sim 50$  was based on assuming  $M_1 \sim 10 M_\odot$ . If the work of Bailyn and coworkers is borne out, then we would need  $\alpha_0 \sim 35$ . To maintain continuity with CCL, however, we keep  $M_1 = 10 M_\odot$  and  $\alpha_0 = 50$ .

Vishniac & Wheeler (1996, hereafter VW; see also Vishniac 1997, hereafter V97) is an important study that provides a framework for understanding the findings of CCL based on considerations of the deviation from steady state flow conditions within the hot, inner part of the accretion disk. Their key insight is that the flow within the hot part of the accretion disk, which exists at small radii during the decay from maximum light after an instability has been triggered, exhibits a deviation from steady state conditions as one approaches the interface with the cold portion of the disk. Their approach to the problem represents a fundamental overthrow of the old idea of expressing the transition front speeds in terms of purely local conditions (Meyer 1984). Part of our motivation in this work is to understand and to test their model.

The CCL model for the limit cycle instability had an advantage over previous studies in that their numerical resolution was much finer than in other models, and they could, through systematic testing, place limits on the extent to which certain aspects of the model could be trusted. In this work, we continue with this line of inquiry by running a series of models based on the numerical code described in previous works (Cannizzo 1993b, 1994; hereafter C93b and C94, respectively; CCL) to investigate various aspects of the model that were studied by CCL. In particular, we study (1) the effects of grid spacing, (2) the analytical model presented by VW, (3) the shape of the outburst versus instability triggering radius, (4) long-term light curves covering quiescence and outburst, both with and without incorporating evaporation of gas from the inner edge of the disk, and (5) the strength of self-irradiation of the outer disk by flux from the inner disk. In the discussion (§ 3), we attempt to synthesize

the lessons that were learned in the previous sections into (somewhat of) a coherent picture of the operation of the limit cycle instability in the BHXBs.

## 2. MODEL CALCULATIONS

For our standard model, we use that presented in CCL. The code has been described extensively (see, e.g., C93b; C94; CCL): it solves explicitly for the time-dependent evolution of surface density,  $\Sigma(r, t)$ , and midplane temperature,  $T_{\text{mid}}(r, t)$ , by simultaneously calculating small corrections in  $\Sigma$  and  $T_{\text{mid}}$  based on the equations of mass and energy conservation. The scalings parametrizing the steady state equilibrium disk structure are given in C93b and CCL and are based on Cannizzo & Wheeler (1984), Meyer & Meyer-Hofmeister (1981), and Pringle, Verbunt, & Wade (1986).

C93b carried out a series of tests using the time-dependent model to determine which terms are dominant and which are less important in their effect on the long-term light curves. They also looked at the effect of varying the number of grid points. The results of the extensive testing done by C93b have been generally confirmed in a recent work that uses a more advanced, time-dependent disk instability code that solves not only the vertically averaged viscous and thermal energy equations but also the radial Navier-Stokes equation and therefore includes radial pressure gradients and departures from Keplerian flow within the transition fronts (Ludwig & Meyer 1998).

We assume a central object mass of  $M_1 = 10 M_\odot$ , a feeding rate into the outer disk of  $3 \times 10^{-11} M_\odot \text{ yr}^{-1}$  (McClintock et al. 1983), a viscosity parameter of  $\alpha = 50(h/r)^{1.5}$ , an inner radius of  $r_{\text{inner}} = 10^7$  cm, and an outer radius of  $r_{\text{outer}} = 10^{11}$  cm. We use a grid spacing of  $\Delta r \propto r^{1/2}$  in §§ 2.2, 2.3, and 2.4 and a spacing of  $\Delta r \propto r$  in §§ 2.1 and 2.5. In the three sections for which  $\Delta r \propto r^{1/2}$ , we take  $N = 1000$  grid points where we look at the properties of individual outbursts, whereas we take  $N = 500$  grid points for the sections that treat complete cycles of outburst and quiescence. For § 2.1, we take  $N = 2^m(10) + 1$ , where  $1 \leq m \leq 5$ , and for § 2.5 we take  $m = 3$  (i.e.,  $N = 81$ ).

### 2.1. Logarithmic Grid Spacing

CCL utilized a grid spacing of  $\Delta r \propto r^{1/2}$ . They discuss earlier time-dependent work by MW, Ichikawa, Mineshige, & Kato (1994; hereafter IMK), and Kim et al. (1994, 1996; hereafter K94 and K96, respectively), in which a logarithmic spacing  $\Delta r \propto r$  is adopted, taking  $N \sim 20$ –40 grid points. Some of the discussion in CCL concerning the number of grid points required to get believable results was speculative in the sense that CCL did not attempt to run models with the logarithmic spacing to substantiate their criticisms, but rather they extrapolated from what they had found using their high-resolution trials. It seems worthwhile to look briefly at this issue of logarithmic grid spacing so as to quantify the requirements for good results. Figure 1 of K94 shows a trial light curve using  $r_{\text{outer}}/r_{\text{inner}} = 10^4$ ,  $M_1 = 3.2 M_\odot$ , and  $\alpha = \alpha_0(h/r)^{1.5}$ . To compare our results more directly with K94, we have generalized our code so that the logarithmic spacing can be used (Cannizzo 1996b).

Figure 1 shows the results of a series of decays for  $N = 21, 41, 81, 161, 321$ , and 501 grid points using the logarithmic spacing. For ease of viewing, the last run was started from different initial conditions so as to be offset slightly from the first five. Several aspects of the decay are apparent. The lower resolution runs have a decay that is too

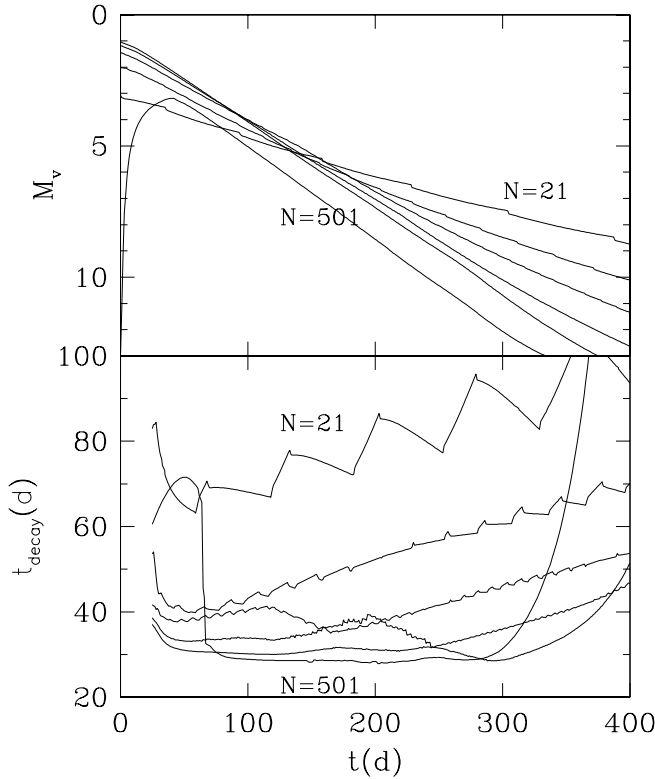


FIG. 1.—Decay from maximum light for a disk initially entirely in the high state but with  $\Sigma(r)_{\text{outer}} < \Sigma_{\text{min}}$  so as to ensure the cooling front starting. We show the light curves in absolute visual magnitude,  $M_v$  (top), and the locally defined decay time constant in days per magnitude (bottom). The six curves are for  $N = 21, 41, 81, 161, 321$ , and  $501$ . The last curve was started from an initial condition with the disk in the low state but with a slight excess in  $\Sigma$  at  $10^9$  (cm) to trigger the instability.

slow. For the  $N = 21$  trial, the decay constant,  $t_e$ , is  $\sim 60$ – $100$  days, whereas in the limit of large  $N$ , we see  $t_e \rightarrow \sim 30$  days. Note also that in the low-resolution runs, one sees glitches in the light curves and  $t_e$  curves associated with the turn off of individual grid points (where “turn off” means the initiation of the cooling transition). Furthermore,  $t_e$  increases with time within a given run for  $N$  small, whereas we know from CCL and VW that for the parameters used, namely  $\alpha \propto (h/r)^{1.5}$ , the decay constant,  $t_e$ , should not vary significantly in time. Therefore, the detailed decay rate in studies such as those mentioned earlier, which used  $N \sim 20$  grid points with the logarithmic spacing, have decays that are spuriously slow by a factor  $\sim 2$ – $3$  and for which the functional form for the decay is more concave upward (i.e.,  $t_e$  increasing with time) than it should otherwise be.

## 2.2. A Close Look at the Cooling Front

CCL present numerous tests of the limit cycle model using  $\alpha = \alpha_0(h/r)^n$  for the Shakura-Sunyaev  $\alpha$  parameter. They show the results of experiments for different values of  $\alpha_0$  and  $n$  and find that for runs with  $n$  close to  $1.5$ , the decays of the outbursts have a nearly exponential form, as required by observations. CCL attempt to understand this result by casting the speed of the cooling front in terms of its width. VW show that this viewpoint is not valid: the width of the cooling front is an artifact of its speed and not the cause. A key part of VW’s insight into the physics of the cooling front and outflow from the hot, viscously evolving part of the

disk is that far away from the front, the local flow speed  $v_r \sim \alpha c_s(h/r)$ , whereas in the front the flow speed  $v_r \sim \alpha c_s$ . VW show how this leads to a front speed of

$$v_f = \alpha_f c_f \left( \frac{c_f}{r_f \Omega_f} \right)^q, \quad (1)$$

where the subscript  $f$  denotes values within the cooling front,  $1/q = 1 + (1 + n/2)[a_1/(1 - nb_1/2)]$ ,  $n$  is the exponent associated with the  $\alpha$  scaling, and  $a_1$  and  $b_1$  are logarithmic derivatives characterizing the steady state scaling associated with the ionized state of the disk,  $a_1 = d \log T/d \log \Sigma$  and  $b_1 = d \log T/d \log \alpha$  (VW; CCL). In other words, the scaling for the midplane temperature associated with the hot disk is  $T_{\text{mid}} \propto \Sigma^{a_1} \alpha^{b_1} r^{-c_1}$ . For the usual Kramer’s law opacity,  $a_1 = c_1 = \frac{3}{2}$  and  $b_1 = \frac{1}{2}$  (C93b; CCL; VW). The midplane temperature associated with the local minimum in the  $\log T_{\text{eff}} - \log \Sigma$  steady state curves is  $T_{\text{min}} \propto \alpha^{-1.1/7} \Omega^{-3/70}$  (VW). Assuming  $\alpha \propto (h/r)^n$  and using the fact that the sound speed in the front,  $c_f$ , is proportional to  $(T_{\text{min}})^{1/2}$ , yields  $d \log T_{\text{min}}/d \log r = [9/140 - (1.1/7)(n/2)]/[1 + (1.1/7)(n/2)]$ . (This last expression, which is eq. [34] of VW, corrects an error in eq. [4] of CCL, namely that the  $r$  exponent should have a positive rather than negative sign. In addition, in eq. [4] of CCL, there should not be a “K” on the right-hand side.)

There are several predictions of the VW theory that are amenable to testing with our time-dependent code. We examine first the evolution of  $v_r/\alpha c_s$  in space and time. Figure 2 shows the variation of the local values of  $v_r/\alpha c_s$  and  $h/r$  with radius for eight time steps spaced 10 days apart during the early decay of a model outburst. The local flow speed is in fact  $\sim \alpha c_s(h/r)$ , the usual viscous flow speed, some distance upstream from the transition front. VW speculate that this point occurs only slightly interior to  $r_f$ , whereas we find it happens at  $\sim (1/2)r_f$ . The derivation of VW is predicated on the fractional disk radius at which this point occurs remaining constant during the decay, which it does. Also, the flow speed does not attain  $\sim \alpha c_s$  at the inner edge of the front, as posited by VW, but rather at the outer edge. At the inner front edge, the flow has only attained a speed of  $\sim (1/6)\alpha c_s$ . [In looking carefully at Fig. 2, one might have imagined a scaling with  $(h/r)^{1/2}$  in the value of  $v_r/c_s$  at the inner edge of the front, but an extension of the run used to generate Fig. 2 in which the cooling front is followed down to  $\sim 10^9$  cm shows that the shoulder in the  $v_r$  curves, which lies at the inner edge of the cooling front, maintains a constant level in terms of  $v_r/c_s$ .] VW note that the results of CCL hinted that  $v_r \sim (1/6)\alpha c_s$  at the inner front edge, and the more detailed model presented by V97 uses this information as a refinement. Figure 3 shows, for the eight time steps indicated in Figure 2, the values of the radii at which the local flow speed goes to zero and the local flow speed equals the standard viscous value  $\alpha c_s(h/r)$ , both given in units of the radius associated with the outermost grid point in the hot state,  $r(i_{\text{hot}})$ . In the early stages of the outburst, the ratio associated with the  $v_r = 0$  radius is  $\gtrsim 0.6$ , but later it approaches a limiting value of  $\sim 0.4$ . The formalism presented in VW, which assumes  $v_r \sim \alpha c_s$  for the flow speed at the inner edge of the cooling front, finds the  $v_r = 0$  fractional radius to be  $\sim 0.23$ , whereas the formalism in V97, which is “corrected” by assuming  $v_r \sim (1/6)\alpha c_s$  at the inner edge of the cooling front, finds the  $v_r = 0$  fractional radius to be  $\sim 0.36$ , in accord with our results. The ratio associated

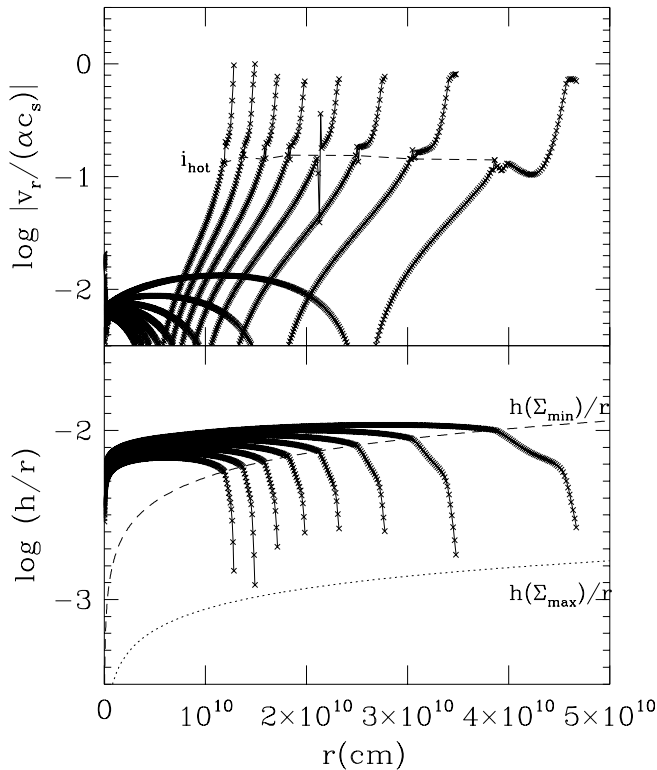


FIG. 2.—Variation in local flow rate and local disk thickness during a decay. The plot shows  $v_f/\alpha c_s$  vs.  $r$  (top) and  $h/r$  vs.  $r$  (bottom). We show eight time steps during the decay spaced 10 days apart as the cooling front moves inward. Crosses indicate individual grid points. The dashed line in the upper panel shows the locus of grid points,  $i_{\text{hot}}$ , that lie at the outermost point of the inner, hot disk. The dashed line in the bottom panel shows the values of  $h/r$  associated with  $\Sigma_{\text{min}}$ , and the dotted line gives conditions at  $\Sigma_{\text{max}}$ .

with the point at which viscous flow is reached asymptotes to  $\sim 0.55$ , which is smaller than that mentioned in VW. The deviations seen in the first few time steps from the limiting values are an artifact of the transitory phase near outburst maximum when the outwardly moving heating front has stopped near the outer disk edge and begun to reflect inward as a cooling wave. This artifact is also seen in the width of the transition front, which is quite broad near the end of the peak of the outburst just as the decay is beginning (see the upper panel in Fig. 5 of Cannizzo 1996c). Last, V97 note that the rate of mass outflow at the front is about 3 times the rate of accretion onto the central object. This is in agreement with Figure 9 of CCL and also with Fig. 2c of C94. In summary, the discrepancies we find with VW are minor, and it seems they have captured the essential physics.

A further prediction of VW is contained within their expression for the cooling front speed. Their formula is more complicated than one might have guessed from the discussion in CCL. One sees, for instance, a dependence on  $a_1$ . From equation (1), we have that  $v_f \propto c_f^{q+n+1} r_f^{(q+n)/2}$ . For the standard model parameters given in CCL and reiterated earlier, the optimal  $n$  value for which  $v_f \propto r_f$  is not 1.5 but rather 1.656. In Figure 4, we show the results of varying  $n$  in much smaller increments than was attempted in CCL. Eleven curves are given corresponding to  $n = 1.50, 1.52, \dots, 1.70$ . Rather than guessing an initial configuration close to outburst maximum and then following the decay, as was

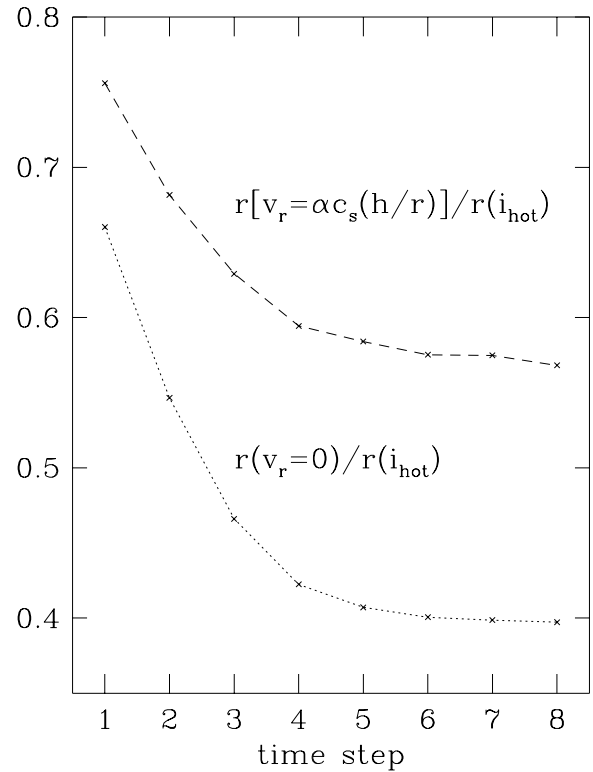


FIG. 3.—Radii at which the local flow speed (1) goes to zero and (2) equals the standard value expected in a steady disk,  $\alpha c_s (h/r)$ . Both are given in units of the radius of the hot portion of the disk,  $r(i_{\text{hot}})$ . The eight time steps shown correspond to those depicted in Fig. 2.

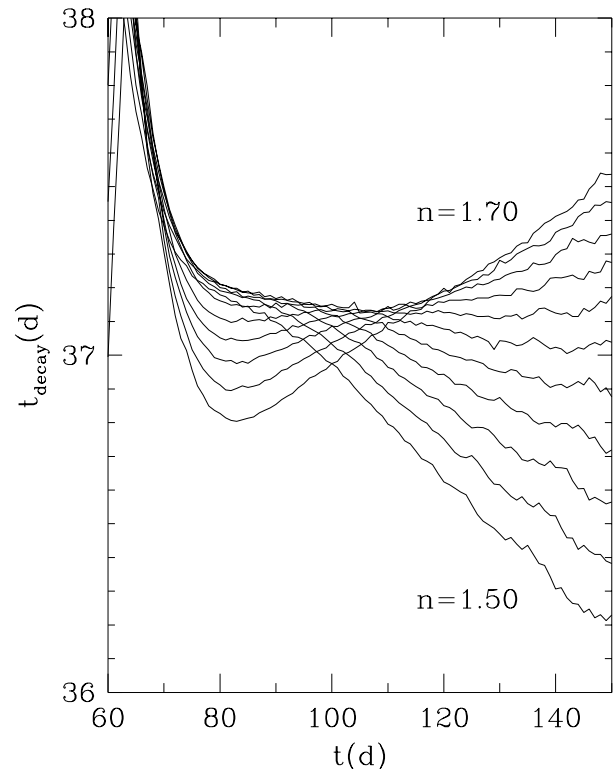


FIG. 4.—Local time constant associated with the decay of the optical flux for eleven values of  $n$ , where  $\alpha = \alpha_0 (h/r)^n$ . The value of  $n$  is 1.50, 1.52, ..., and 1.70. To keep the value of  $M_v$  within a common range, the proportionality constant,  $\log \alpha_0$ , is varied in steps of 0.04 from 1.7 to 2.1.

done in CCL, here we initiate an outburst at a small radius and wait until the disk has gone nearly entirely to the high state and then begun its decay. In this manner, the disk adjusts to its desired state as the outburst decay starts, and we are not left with a long transient near the beginning of the decay as in CCL. In Figure 4 we see that, contrary to the discussion given in CCL,  $n = 1.5$  does not yield a precisely exponential decay. Our optimal value is about 1.63, which is close to the value 1.656 given by VW's analytical formalism. Note the small dynamic range in  $e$ -folding times represented along the  $y$ -axis. The observational uncertainties and intrinsic source fluctuations would probably not allow one to distinguish among the range of  $n$  values shown here, so this result is not of direct relevance observationally. The motivation is solely to confirm VW. It would be a worthwhile exercise to analyze the decays of dwarf novae and X-ray novae in a consistent fashion to see how precise of a constraint one may be able to place on  $n$ , or, more broadly, how essential is the functional form  $\alpha = \alpha_0(h/r)^n$ .

For completeness, we show in Figure 5 the variation of the width of the front during the rise and decay of an outburst. The outburst begins at a small radius, so we see first the outward propagation of the heating front, then the inward movement of the cooling front. As noted by CCL, the width of the cooling front can be approximated by  $w \simeq (hr)^{1/2}$  or  $w/r \simeq (h/r)^{1/2}$ . VW show that both the cooling front width and speed of propagation are set by the departure from steady state discussed earlier and are not causally linked. It is interesting that the fractional width of the outward-moving heating front is given phenomenologically

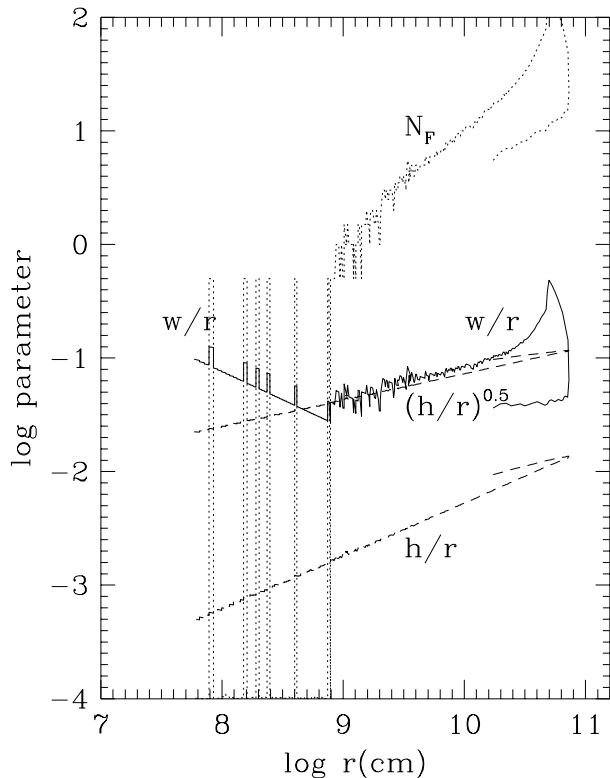


FIG. 5.—Variation of properties associated with the transition front during an outburst that is triggered at a small radius. We show the number of grid points with the front,  $N_F$ , the fractional width of the front,  $w/r$ , and the ratios,  $(h/r)^{1/2}$  and  $h/r$ , evaluated in the outermost radial zone within the hot state. Within the rise of the outburst,  $w/r \sim (h/r)^{0.75}$ , whereas during the decay,  $w/r \sim (h/r)^{0.5}$ .

by  $w/r \simeq (h/r)^{0.75}$ . Ludwig & Meyer (1998) find somewhat broader heating fronts. Their Figure 14 is interesting because it plots the heating and cooling front velocities versus radius on a common scale. VW put forth an analytical theory for the period of decaying light associated with the inward-moving cooling front; no such theory currently exists for the period of rising light associated with the outward-moving heating front. The sharp spike in  $\Sigma$  accompanying the heating waves is caused by the high-viscosity material pushing into the region of lower viscosity material (Lin, Papaloizou, & Faulkner 1985). The fact that it is narrower than the cooling front must be an artifact of this pushing, but further work will be needed to determine a valid numerical parametrization of the speed in order to lead ultimately to a successful theory of the heating front.

### 2.3. Outburst Light Curve versus Triggering Location

It has been known for some time that, within the context of the limit cycle model, outbursts triggered near the inner edge of the disk tend to show slow rise times, while outbursts triggered at somewhat larger radii generate faster rise times (Smak 1984; Cannizzo, Wheeler, & Polidan 1986, hereafter CWP). The reason for the difference in rise times is detailed in CWP. For most of the bright BHXB outbursts, one sees fast rise times (of order a few days) in outbursts lasting  $\sim 100$ – $200$  days. It is therefore of interest to find the minimum critical radius such that a fast rise will be obtained. Figure 6 shows a series of outbursts generated by starting with a smooth  $\Sigma(r)$  distribution resembling that expected at the end of the quiescent (i.e., accumulation)

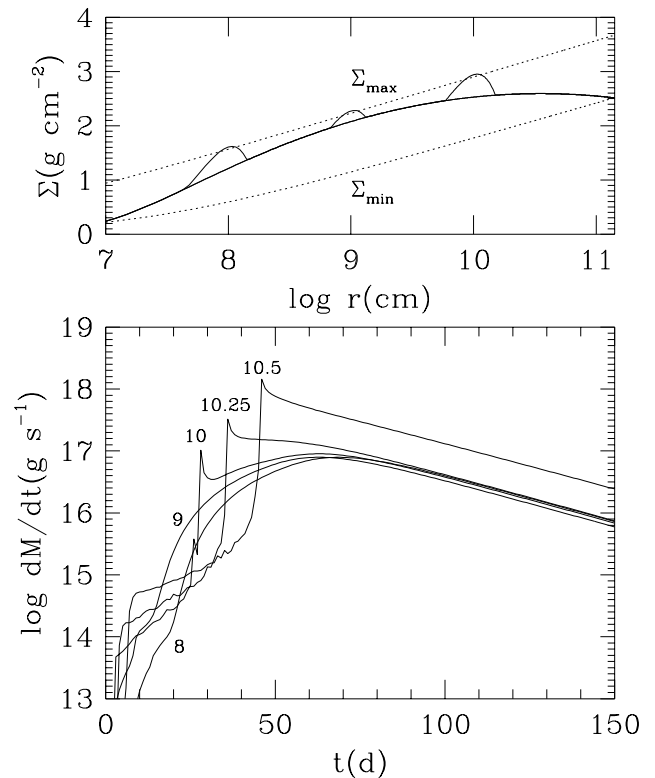


FIG. 6.—Dependence of the outburst profile on the radial location of triggering. *Top*: Initial low state configuration; *bottom*: resulting light curves. The three small Gaussians in the top panel are representative of the narrow surface density enhancements that are added to the broad, underlying configuration, in order to trigger the outburst. The functional forms of the narrow and broad Gaussians are given in the text.

phase and adding to this profile a small spike whose maximum exceeds the local value of  $\Sigma_{\max}$ . This is carried out by superposing two functions, as shown in the top panel of Figure 6. The functions are

$$S_{\text{broad}} = 0.7\Sigma_{\max} \exp\left(\frac{-\{\log[r(\text{cm})] - \log[r_{\text{mid}}(\text{cm})]\}^2}{2}\right) \quad (2)$$

and

$$S_{\text{narrow}} = 1.1\Sigma_{\max} \exp\left[\frac{-(r - r_{\text{center}})^2}{2w^2}\right], \quad (3)$$

where  $r_{\text{mid}} = 10^9$  cm is the geometric average of the inner and outer radii,  $r_{\text{center}}$  is the central radius of the narrow Gaussian used to trigger the outburst,  $w = r_{\text{center}}/3$ , and  $\Sigma_{\max}$  is the local maximum in  $\Sigma$  from vertical structure computations (Cannizzo & Wheeler 1984). For a given trial, we prescribe the initial surface density distribution by taking  $\Sigma(r) = \max(S_{\text{broad}}, S_{\text{narrow}})$ . Five trials were run, corresponding to  $\log r_{\text{center}}(\text{cm}) = 8, 9, 10, 10.25$ , and  $10.5$ . (For ease of viewing, we do not show the 10.25 and 10.5 curves in the top panel of Fig. 6.) Note the stark difference in the rise time properties between the first two and last three curves. The rise is slow for the  $\log r_{\text{center}}(\text{cm}) = 8$  and  $9$  curves, whereas it is fast for the  $\log r_{\text{center}}(\text{cm}) = 10, 10.25$ , and  $10.5$  curves (see also Cannizzo 1996b). The instability is triggered at  $t = 0$  for all five trials, but because of the finite travel time of the heating front, the effect of increased viscosity and mass flow rate is not felt at the inner disk until  $\sim 30$ – $50$  days later for the three trials with triggering at large radii, whereas the effect is felt much sooner for the trials triggered at small radii. The difference in the heating wave properties is shown in Figure 7. The two panels show the evolution of surface density, in 5 day steps, for the  $\log r(\text{cm}) = 9$  and  $10$  runs. These two span the transition region of parameter space between slow and fast rise. For the outbursts triggered at large radii, the amplitude of the outburst is larger because more mass is contained within the wave of surface density enhancement associated with the heating front. The slow rise times associated with the  $\log r(\text{cm}) = 8$  and  $9$  curves are caused by the fact that, to enhance appreciably the rate of mass flow at the inner disk edge, the outwardly traveling heating front must access the bulk of the matter that is stored in the disk at large radii, between the Lubow & Shu (1975) radius (corresponding to that point in the disk where the specific angular momentum associated with the gas leaving the L1 point at the surface of the secondary star equals the Keplerian value in the disk) and the outer disk edge, and this matter, after having made the transition from neutral to ionized gas, then has to viscously evolve (to both smaller and larger radii). The physics associated with this flow is discussed in CWP and C93a.

#### 2.4. Long-Term Light Curves

As noted by many authors, the standard limit cycle model fails to account for observations of systems in quiescence (see Lasota 1996a, 1996b). One observes a significant EUV and X-ray flux that we infer to be the result of accretion during quiescence, and yet, if we are to take the theory literally, it predicts a quiescent accretion rate that is negligibly small. The small accretion rate is mandated by the requirement that  $\Sigma < \Sigma_{\max}$  and  $T_{\text{eff}} < T_{\text{eff}}(\Sigma_{\max})$  for all radii,

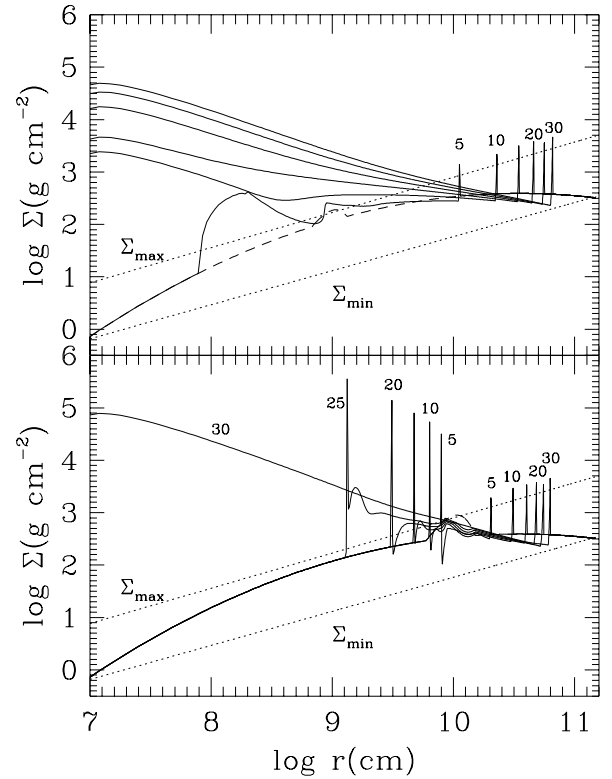


FIG. 7.—Variation of the surface density with radius and time for inside-out and outside-in outbursts. We show a model run for  $\log r_{\text{center}}(\text{cm}) = 9$  and for  $\log r_{\text{center}}(\text{cm}) = 10$ . The dashed curve gives the initial state, which is entirely along the lower branch of the S-curve, and dotted lines correspond to the local maxima and minima in  $\Sigma$  from the steady state scalings. We show 30 days of evolution, with a 5 day spacing between each curve. In the top panel, there are six sharp spikes evident between  $\log r(\text{cm}) = 10$  and  $11$  showing the outward movement of the heating wave at  $t(\text{days}) = 5, 10, 15, 20, 25$ , and  $30$ . In the lower panel, there are also six spikes in a similar radial range showing the outward movement, as well as five spikes between  $\log r(\text{cm}) = 9$  and  $10$  showing the movement of the inner edge of the heating front at  $t(\text{days}) = 5, 10, 15, 20$ , and  $25$ . For  $t(\text{days}) = 30$ , the hot region extends all the way down to  $\log r(\text{cm}) = 7$ .

in particular  $r \sim r_{\text{inner}}$ . McClintock, Horne, & Remillard (1995) found evidence for low-level accretion of  $\sim 10^{10}$ – $10^{11}$   $\text{g s}^{-1}$  (if the efficiency of accretion,  $\epsilon$ , is approximately 0.1) in the quiescent state of A0620–00, but this is still much greater than would be allowed in the “pure” version of the standard accretion disk model in which the inner disk edge extends all the way to the last stable orbit (Lasota, Narayan, & Yi 1996). The critical accretion rate associated with  $\Sigma_{\min}$  is  $\dot{M}(\Sigma_{\min}) \sim 10^6 \text{ g s}^{-1} (r_{\text{inner}}/10^7 \text{ cm})^{2.6}$  for BHXBs (CCL). There is nothing in the model, however, that requires  $r_{\text{inner}} = 6GM_1/c^2$ . Time-dependent computations of the accretion disk limit cycle instability have shown that the model still works well if the inner edge is truncated (see, e.g., Angelini & Verbunt 1989; C93b). There may exist some physical mechanism extrinsic to the standard limit cycle model that serves to evaporate or take material from the inner disk and transfer it more or less directly onto the accretor (see, e.g., Meyer 1990; Meyer & Meyer-Hofmeister 1994; Liu et al. 1995). Such a mechanism may or may not fit in with the general paradigm of accretion onto black holes (Chakrabarti 1996a, 1996b; Narayan, McClintock, & Yi 1996). Workers are beginning to consider the effect such a process would have on the limit cycle model in terms of how

the altered surface density distribution in quiescence—in particular, the lack of an inner disk—would change the properties of the outburst (Lasota et al. 1996; Hameury et al. 1997, hereafter HLMN).

When we run complete cycles using the  $\alpha = 50(h/r)^{1.5}$  scaling, we find frequent outbursts that are triggered at small radii and that have slow rise times, in contrast to the observations. If the inner disk were missing because of a slow removal of matter onto the accretor, then the outburst would have to be triggered farther out. This may not be a unique solution to the problem, and at least three obvious alternatives are apparent. (The problem of the quiescent X-ray flux would only be addressed by the third option.)

1. The constraint imposed by observed exponential decays,  $\alpha = 50(h/r)^{1.5}$ , is actually only applicable to the matter that resides in the “hot state” part of the disk. Once the matter has made the transition to the low state, it does not participate in the flow dynamics. Therefore, it is quite probable that  $\alpha = 50(h/r)^{1.5}$  is a scaling that applies only to ionized gas at  $T > 10^4$  K, and for neutral gas at  $T < 10^4$  K, there may be another scaling that drops  $\alpha$  abruptly to a value less than  $50(h/r)^{1.5}$ . In this case, the material would evolve less in quiescence, and there would be less tendency for the matter to spread and trigger an inside-out outburst with its attendant slow rise.

2. We have not yet activated and tested the section of our code that provides for a variable outer disk radius (see Ichikawa & Osaki 1992). The qualitative effect this has on the evolution is to sweep up matter at large radii, which shrinks the outer disk in quiescence. The contraction is caused by the accretion of low angular momentum material. This has the effect of enhancing the surface density near  $r_{\text{outer}}$  and leaving the disk more prone to outbursts triggered at large radii (see Ichikawa & Osaki 1994).

3. There may exist a mechanism that prevents the cooling wave from propagating once it reaches some radius,  $r_{\text{crit}}$ . Since  $\dot{M}_{\text{min}}(r) = \dot{M}(\Sigma_{\text{min}})$ , which provides a measure of the quiescent mass flow rate at a radius  $r$ , scales as  $\sim r^{2.6}$ , if  $r_{\text{crit}}$  were at  $\sim 10^9$ – $10^{10}$  cm, for example, this would be sufficient to leave a small, hot inner disk in quiescence that could give rise to the quiescent X-rays at a level  $\sim 10^{10}$ – $10^{11}$  g s $^{-1}$  seen in A0620–00 using a standard accretion efficiency of  $\epsilon \sim 0.1$ .

Having made these concessions, we must return to our original point that the EUV/soft X-ray observations seem to demand some evaporation of the inner disk (unless the third option just discussed turns out to be true). Although we are uncertain of the physics that leads to evaporation, we should include at least an ad hoc prescription for removal of matter from the inner disk in any complete time dependent model. We therefore evacuate matter from the inner disk through the prescription  $\partial\Sigma(r)/\partial t = -\Sigma_0/[1 + (r/r_0)^2]^2$ , where  $\Sigma_0 = 10^2(M_1/M_\odot)^{-1}$  g cm $^{-2}$  s $^{-1}$  and  $r_0 = 100r_g = 2.95 \times 10^7(M_1/M_\odot)$  cm (R. Narayan 1996, private communication). This gives an integrated mass removal of  $\dot{M}_{\text{evap}} = -\int (\partial\Sigma/\partial t) 2\pi r dr = \pi\Sigma_0 r_0^2/[1 + (r_{\text{inner}}/r_0^2)] = 2.7 \times 10^{17}$  g s $^{-1}$   $[1 + (r_{\text{inner}}/r_0^2)]^{-1}$  ( $M_1/M_\odot$ ). We must have some matter at each grid point for our code to work properly; therefore, when  $\Sigma$  drops below 1 g cm $^{-2}$  at a given radius, we set it equal to 1 g cm $^{-2}$ .

Figure 8 shows a series of light curves with and without evaporation. We use the expression given in the previous

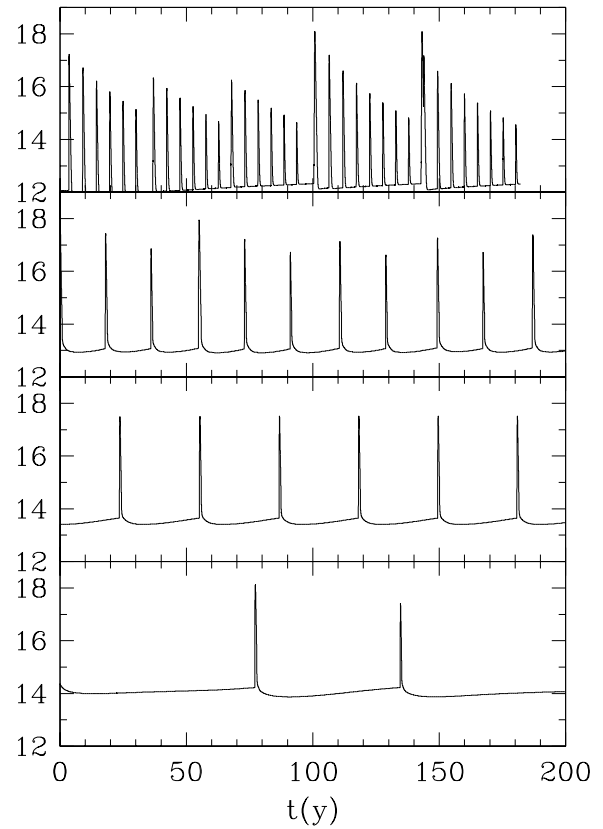


FIG. 8.—A series of outbursts spanning several cycles of quiescence and outburst. The y-axis shows the log of the mass accretion rate from the innermost grid point in grams per second, and the x-axis gives the time in years. The top panel represents the standard model without evaporation. For the next three panels, we remove material from the inner edge of the disk at the rate given in the text, with the normalization constant given in the text multiplied by  $10^{-x}$ , where  $x = 4, 3$ , and  $2$  (from top to bottom).

paragraph for  $\dot{M}_{\text{evap}}$ , with the normalization multiplied by  $10^{-x}$ . For the four panels shown,  $x = \infty, 4, 3$ , and  $2$ . Hence, in the top panel, we present our standard model without evaporation. Outbursts are triggered frequently—about every 5 years—at small radii in the disk. Most of the outbursts have fairly low amplitude, but since the 1975 outburst of A0620–00 made it a sustained  $\sim 50$  Crab source in 3–6 keV X-rays as seen by *Ariel 5* (Elvis et al. 1975), the fainter outbursts produced in our “standard” model would have been seen over the past  $\sim 20$  years, had they occurred. About every 50 years, we get a major outburst in the models. The introduction of evaporation removes the inner parts of the disk, eliminates the minor outbursts, and increases the recurrence times for the major outbursts. Figure 9 shows the mass of the accretion disk accompanying the runs shown in Figure 8. During a major outburst, a fraction,  $\sim 0.2$ , of the disk is accreted, whereas during a minor outburst,  $\lesssim 0.01$  of the disk is accreted.

Figure 10 shows expanded views of one major outburst taken from each of the four panels in Figure 8. The quiescent values of the accretion rate in third panel of Figure 10 show the effective rate of the evaporation or mass loss from the disk. In the models of Narayan et al. (1996) and Esin, McClintock, & Narayan (1997), for instance, the efficiency of accretion is low in the quiescent state,  $\epsilon \sim 10^{-4}$ , while in outburst one still has  $\epsilon \sim 0.1$ . Therefore, one would see a greater dynamic range in soft X-ray flux between quiescence

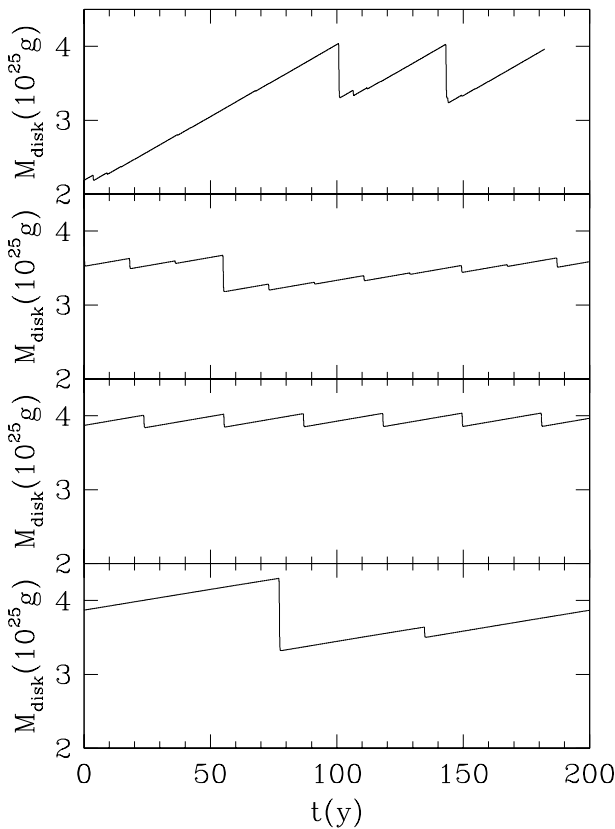


FIG. 9.—Time history of the mass of the accretion disk accompanying the four light curves shown in Fig. 8.

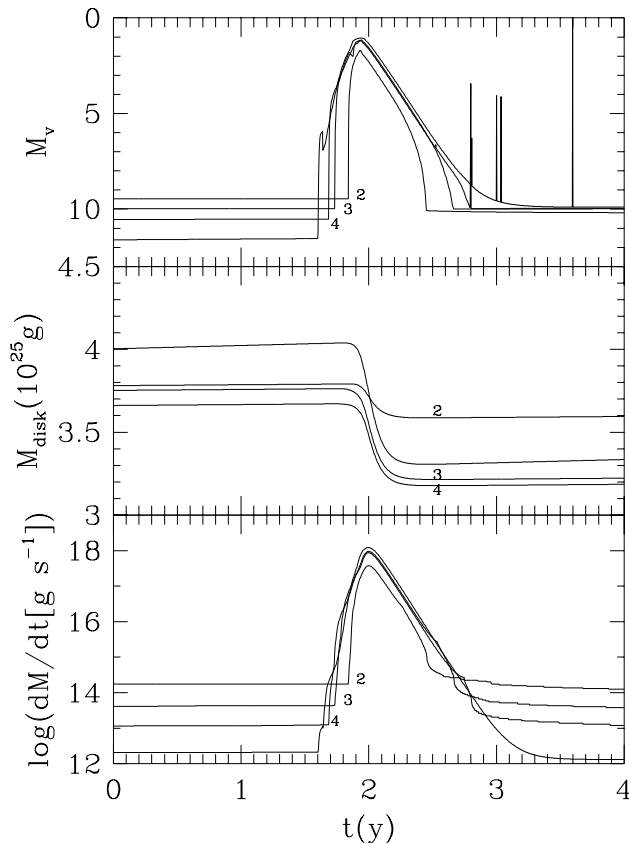


FIG. 10.—One major outburst taken from each of the four panels in Fig. 8. The values of  $x$  are given beside each curve. Smaller  $x$  values correspond to larger evaporation.

and outburst than would be inferred directly from the rates of accretion given in Figure 10. Also, our condition that  $\Sigma(r) \geq 1 \text{ g cm}^{-2}$  reduces the effective rate of evaporation increasingly for smaller  $x$  values (i.e., higher evaporation rate): the effective evaporation rates in going from  $x = 4$  to  $x = 2$  increase by a factor of  $\sim 5$  for each of the two factor of 10 increases in  $10^{-x}$ .

In Figure 10 we see that, as expected, the fact that triggering of outbursts cannot occur at small radii because of the truncation of the inner disk forces the rise times to shorten. Even for the highest values of  $\dot{M}_{\text{evap}}$ , however, the rise times are  $\sim 1$  month—longer than the value of several days commonly seen. For low values of the evaporation, only the quiescent surface density profile is affected. The reason the outburst  $\Sigma(r)$  profile is not strongly changed is that during outburst, the surface density near the inner edge is so large that the local mass flow greatly exceeds the local evaporation rate. In looking at the decays of the outbursts in the last panel of Figure 10, however, we see that for a high evaporation rate, the outburst itself is also affected: the decay is cut off so that the exponential decay is truncated. This occurs because at some point during the inward movement of the cooling front, there is no longer any disk left into which the cooling wave may propagate. For instance, for  $x = 2$ , we only observe about two decades of exponential decay in the value of  $\dot{M}$  at the inner edge, which presumably powers the soft X-ray flux we observe. In systems like A0620–00, however, we observe about three decades of exponential decay (Tanaka & Shibazaki 1996). The model with  $x = 2$  corresponds to  $\dot{M}_{\text{evap}} \sim 2 \times 10^{14} \text{ g s}^{-1}$ , with our standard assumed secondary star mass transfer rate value,  $\dot{M}_T$ , approximately equal to  $2 \times 10^{15} \text{ g s}^{-1}$ . The rise time is  $\sim 1$  month. The rise time could be shortened presumably by increasing  $\dot{M}_{\text{evap}}$  further (i.e., decreasing  $x$ ), but that would reduce the dynamic range of the soft X-ray flux accompanying the exponential decay to an even more unacceptably small value.

Figure 11 shows the evolution of  $\Sigma$  and  $T_{\text{mid}}$  covering an outburst in the third panel of Figure 8. There are 10 time steps shown, with the first time step corresponding to just before the triggering of the outburst. The time increment,  $\delta t$ , equals 0.1 yr. The starting time step shows the truncated nature of the disk due to evaporation. The outburst triggers at  $\log r(\text{cm}) \sim 9.6$ . In the early stages of the outburst, evaporation does not have any effect on the outburst, as the  $\Sigma(r)$  values are quite large for  $r$  small. In looking at time steps 8, 9, and 10, however, we see that in the late stages of the outburst when  $\Sigma(r)$  becomes smaller, the evaporation swallows up the last of the inner, hot disk before the cooling front can propagate all the way to the inner edge. In time step 8, for instance, the hot disk exists only in a ring from about 8.5 to 9.5 in terms of  $\log r(\text{cm})$ . For time steps 9 and 10, the entire disk is back into the low state. This leads to the truncation of the full exponential decays evident in Figure 10. Figure 12 reveals the evolution in quiescence by showing four time steps that follow the last profile in Figure 11, here taking  $\delta t = 10$  yr. One can see evaporation eating into the quiescent  $\Sigma(r)$  distribution, even as matter in the inner disk evolves viscously, and matter at the outer edge continues to arrive from the secondary star.

In summary, evaporation appears not quite capable, at least for a system with parameters relevant for a system like A0620–00, of producing outbursts that occur at large enough radii to give rise times that are as fast as observed



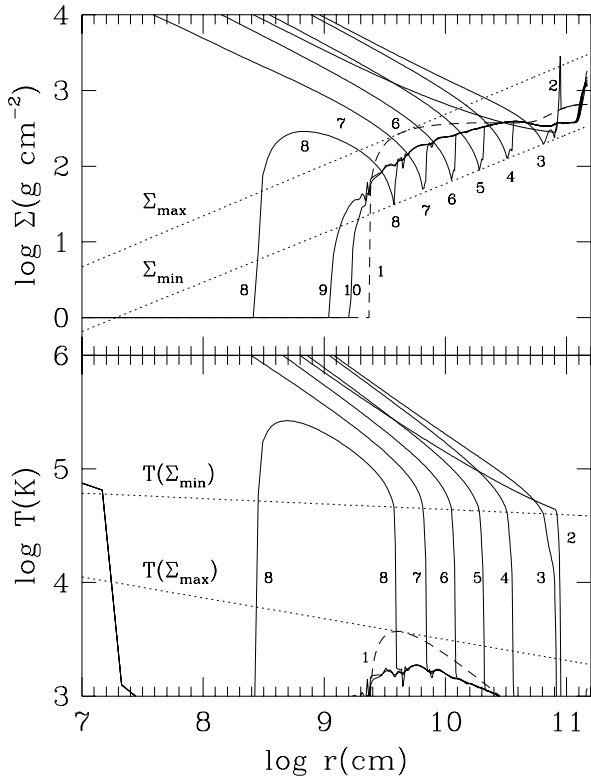


FIG. 11.—Evolution of  $\Sigma$  and  $T$  accompanying an outburst in the third panel of Fig. 8. Ten time steps are shown, with the first corresponding to just before an outburst begins. There is a spacing of 0.1 yr between curves. The high temperature at the inner disk edge is an artifact of our imposition that  $\Sigma(r) \geq 1 \text{ g cm}^{-2}$ , which prevents the inner edge from cooling completely.

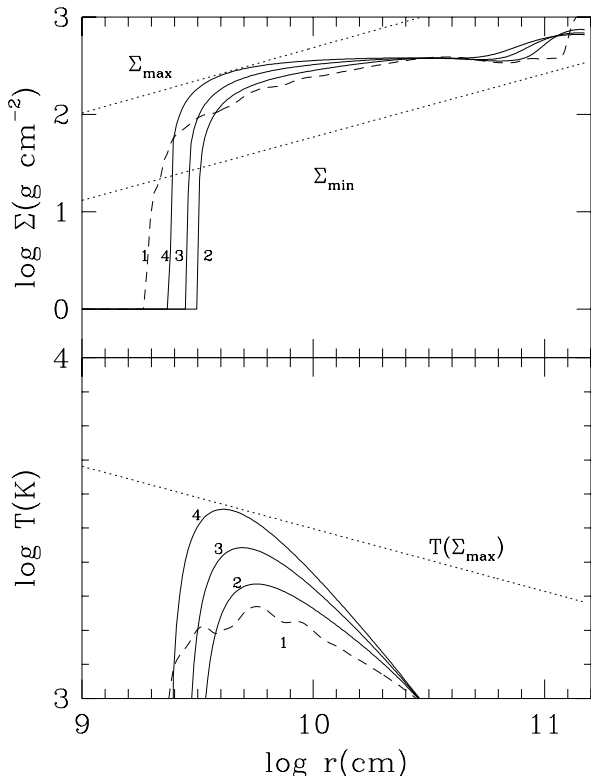


FIG. 12.—Evolution of  $\Sigma$  and  $T$  continuing from Fig. 11, showing the quiescent period following the outburst. The first time step corresponds to the last step in Fig. 11. Four time steps are shown, and the spacing is 10 yr.

and that simultaneously have  $\sim 2\text{--}3$  decades of exponential decay. Since the models are so close to working, one could argue that, given the crude nature of the models, we could consider this a qualified success. On the other hand, evaporation unquestionably does help in the standard model as regards the recurrence times for outbursts. The effect or necessity of evaporation in the models may potentially be different for other model parameters, for instance with systems for larger orbital periods and higher  $\dot{M}_T$  values. HLMN find, for example, that evaporation is needed to obtain light curves in various energy bands that can account for observations of the start of an outburst seen in GRO J1655–40, a system with a much longer orbital period,  $P_{\text{orbital}} = 2.6$  days (Bailyn et al. 1995), and a higher mass transfer rate,  $\dot{M}_T = 2 \times 10^{17} \text{ g s}^{-1}$ , than we have assumed in this work for our standard model ( $P_{\text{orbital}} = 7.75$  hr, giving  $r_{\text{outer}} = 1.5 \times 10^{11} \text{ cm}$  and mass transfer rate  $\dot{M}_T = 1.89 \times 10^{15} \text{ g s}^{-1}$ ) taken to be representative of A0620–00. HLMN do not show light curves covering complete cycles of quiescence and outburst, so it is difficult to assess the full generality of their conclusions. In particular, it may prove difficult for any disk instability model to reproduce the prompt decay in  $V$  that was seen in *Hubble Space Telescope* observations that occurred even as the 2–10 keV X-ray flux was increasing for the 1996 outburst in GRO J1655–40 (Hynes et al. 1996). The fact that the two microquasars do not show the classical fast rise, exponential decay outburst may be associated with the fact that the black holes (BHs) in these systems seem to be maximally rotating (Zhang, Cui, & Chen 1997). Our results do not support the strength of the contentions of HLMN about the necessity of evaporation. Preliminary work using our canonical SS Cygni model (C93b; Cannizzo 1996c, 1998c) also finds evaporation to be ineffectual in bringing about fast rise outbursts for models that are intrinsically prone to slow rise outbursts. Cannizzo (1998c) finds that, even in the limit where  $\dot{M}_{\text{evap}} \rightarrow \dot{M}_T$ , the outburst rise times as taken from light curves computed using  $\dot{M}_{\text{inner}}$  are still slower than the fast rise outburst in SS Cygni observed by Mauche (1996) in the EUV. One could not of course have  $\dot{M}_{\text{evap}} = \dot{M}_T$ , or the entire disk would evaporate.

### 2.5. Strength of the Irradiation

Tuchman et al. (1990) present a formalism for incorporating the effects of irradiation on the equilibrium structure of the disk determined by the vertical structure calculations. We have included their formalism into our time-dependent model to calculate the local irradiation temperature and its effect in altering the S-curve. In this preliminary work, we only activate the portion of the code that calculates the irradiation temperature. We leave for future work a computation that includes its feedback into the structure of the disk.

Shakura & Sunyaev (1973) give the local irradiation flux as

$$F_{\text{irr}} = C \frac{L_X}{2\pi r^2}, \quad (4)$$

where  $C = Ad(h/r)/d \ln r$ ,  $n = 1$  for neutron star accretors, and  $n = 2$  for black hole accretors. The parameter  $A$  is the X-ray albedo. The values of  $n$  advocated by Shakura & Sunyaev are based on the supposed preferred directions for the emission: isotropically from the neutron star surface

( $n = 1$ ) and primarily vertically from the disk surface for black hole primaries ( $n = 2$ ). One cannot claim to understand the emission geometry at small radii in the BHXBs—for instance, there may exist a scattering medium above the disk that influences the value of  $n$ —so, therefore, we show results for both  $n = 1$  and 2 as being representative of possible values.

Figures 13 and 14 show the values of ratios of the locally defined irradiation temperature,  $T_{\text{irr}} = (F_{\text{irr}}/\sigma)^{1/4}$ , to the local (viscous) effective temperatures for 600 days of evolution with  $\delta t = 6$  days spanning the rise and decay of an outburst in the standard model. We show  $n = 1$  and  $n = 2$  and assume  $A = 1$ . As in § 2.1, we adopt a logarithmic grid spacing so as to resolve better the inner portions of the disk. We take  $N = 81$  grid points. For the case  $n = 2$ , which is thought to be more representative of the BHXBs, the local irradiation temperature is never more than about 0.3–0.4 of the local effective temperature determined from equating viscous heating and radiative cooling. This occurs near the time of maximum light in the outburst. Van Paradijs (1996) presents revised criteria for the allowability of the limit cycle mechanism in the soft X-ray transients (SXTs), including neutron star and black hole systems. He concludes that irradiation is more effective for neutron star accretors than for BHXBs at preventing the limit cycle from operating by virtue of keeping the entire disk in the ionized state. In his Figure 2, he indicates that A0620–00 lies a factor of  $\geq 10$  below the dividing line between steady and unsteady behavior. Therefore, our finding of relatively weak irradiation for a model meant to represent A0620–00 is consistent with the fact that A0620–00 has exhibited two outbursts (in 1917 and 1975) and is seemingly not prone to irradiation-

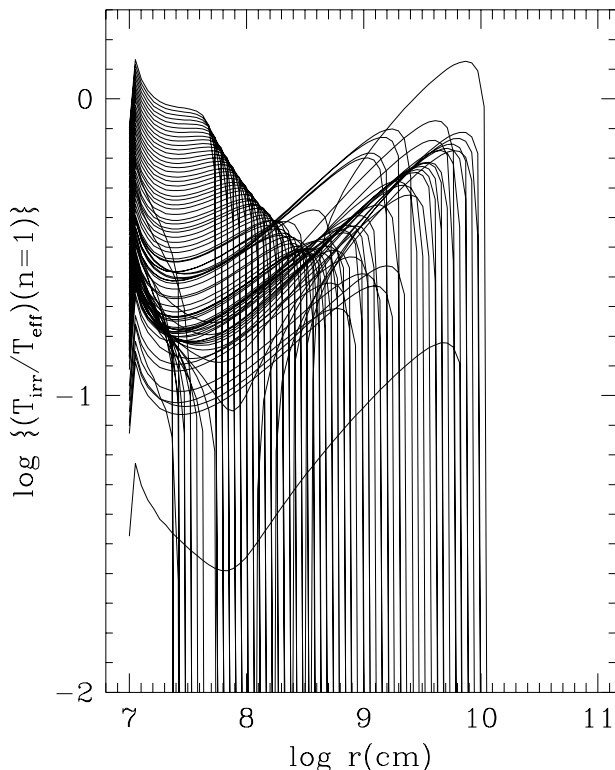


FIG. 13.—Ratio of the local irradiation temperature to the local effective temperature for 600 days of evolution, shown at 6 day intervals, for  $n = 1$ . The dropoff at large radii moves inward as time progresses.

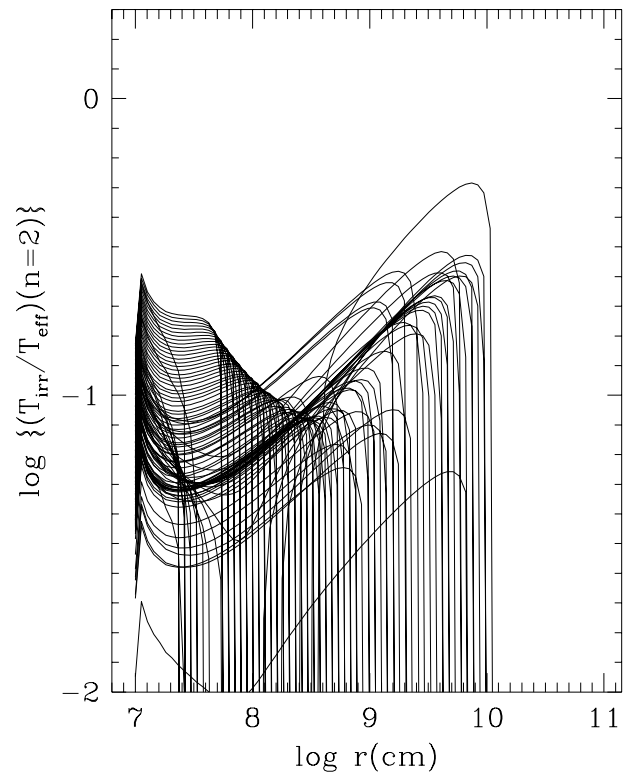


FIG. 14.—The ratio of the local irradiation temperature to the local effective temperature for 600 days of evolution, shown at 6 day intervals, for  $n = 2$ . The dropoff at large radii moves inward as time progresses.

induced effects. It is also consistent with HW and MW who found, by comparing theory with observation for A0620–00, that irradiation does not contribute overwhelmingly to the optical flux.

### 3. DISCUSSION

We have investigated a variety of phenomena associated with the limit cycle model as it may apply to the BHXBs. We find the following:

1. The grid spacing in which  $\Delta r \propto r$  does not appear to be as convenient as the spacing  $\Delta r \propto r^{1/2}$  because the former overresolves the innermost part of the disk, resulting in long CPU times for execution. Low-resolution runs with  $N \simeq 20$ –40 grid points produce light curves that show artificial “steps” in the decay caused by the turnoff of individual grid points. In addition, the locally defined  $e$ -folding decay times are too slow by  $\sim 2$ –3, and the decay character is artificially slower than exponential. As  $N$  is made to increase, the steps become smaller and disappear, and the decay timescales asymptote to a common value, as expected in a numerical scheme that converges properly. We have only investigated properties associated with the decay. There may be other spurious systematic effects associated, for instance, with the long-term light curves (i.e., the triggering radii and outburst rise times) or with the production of reflare or spikes in the light curve (see, e.g., K96), which would be smoothed out in a much higher resolution model.

2. The light curves for outbursts have slow rise times when triggered at radii  $\lesssim 10^9$  cm in the disk and fast rise times when triggered at radii  $\gtrsim 10^{10}$  cm. There is an abrupt change in the character of the rise at some radius interme-

diate between these two values. In this context, it is somewhat of a misnomer to refer to the two cases as “inside-out” and “outside-in,” since, in both instances, the triggering radius is much less than the outer disk radius. The outburst light curves of interest in this work are typified by A0620–00 and show not only an exponential decay with  $\sim 30$ – $40$  day  $e$ -folding timescale but also a fast rise (i.e., several days). These experiments in which we artificially trigger the outbursts at a specific radius show that, to produce outbursts with rise times as fast as those observed, the triggering radius must be at least as large as some value between about  $10^9$  and  $10^{10}$  cm, for A0620–00 parameters.

3. The model of VW for the decay of the outburst, based on considerations involving a deviation from steady state flow in the inner part of the disk, is substantially borne out in detailed testing. Their basic premise is that the local flow speed “accelerates” from the local value of  $\alpha c_s(h/r)$  to the local value of  $\alpha c_s$  within the hot part of the disk. VW conceive of the point at which  $v_r \sim \alpha c_s$  is attained as being at the inner edge of the cooling transition region, whereas we find it to be at the outer edge. This does not have an impact on VW’s derivation. More importantly, we find that the value of the radius at which  $v_r$  changes sign, expressed in units of  $r(i_{\text{hot}})$ , asymptotes to  $\sim 0.4$ , whereas the fractional radius at which the local flow rate equals the standard viscous flow rate asymptotes to  $\sim 0.55$ .

The work of CCL had as its underlying premise the assumption that the decay of the soft X-ray flux in the outbursts seen in the BHXBs is caused by a cooling wave. With that as a working hypothesis, CCL showed that  $\alpha_{\text{hot}} \sim 50(h/r)^{1.5}$  is needed, and the  $e$ -folding decay time for  $dM/dt$  is  $\sim 0.4(GM_1/\alpha_0)c_s^{-3}$ , where  $c_s \sim 16 \text{ km s}^{-1}$ . An alternative starting point, advocated recently by King & Ritter (1998), is that the decays in the BHXB outbursts are due to the gradual loss of disk material into the BH. The cooling wave is unable to start because of strong irradiation, and so the hot, viscous disk can only lose material from its inner edge. Cannizzo, Lee, & Goodman (1990) showed that, for  $\alpha$  constant,  $dM/dt$  decreases in a purely viscous disk as  $\sim t^{-1.3}$ . To get an exponential decay as observed, the kinematic viscosity coefficient,  $\nu \propto \alpha T_{\text{mid}}$ , must be constant, implying either an isothermal disk with  $\alpha$  constant or else  $\alpha \propto 1/T_{\text{mid}}$ . Neither option seems physically reasonable. It is interesting that for both the cooling wave model and the viscous decay model, a constant  $\alpha_{\text{hot}}$  value does not work (Cannizzo 1998b). Mineshige, Yamasaki, & Ishizaka (1993) pointed out that purely viscous decays lead to power law light curves and that a cooling wave that extracts mass and angular momentum from the hot, viscous disk can produce the required exponential decay. They present a toy model in which  $\partial\Sigma/\partial t \propto -\Sigma/t_0$  is put in by hand, rather than determining a form for  $\alpha_{\text{hot}}$  that will lead to the exponential process self-consistently using a full time-dependent model, as in CCL. King & Ritter (1998) point out that the constraints on the functionality of  $\alpha$  derived from arguments like those presented in Cannizzo et al. (1990) do not apply for disks in which the midplane temperature is determined not by viscous heating but rather by irradiation. For the midplane temperature to be strongly influenced, a rather large irradiation is needed (Tuchman et al. 1990). Our estimate that  $T_{\text{irr}} \sim 10^4 \text{ K}$  at the outer disk edge may be unrealistically low. During the time in which the optical flux decreased by  $\sim 2$ – $3$  mag in the 1975 outburst of A0620–00, the X-ray flux fell by a factor  $\sim 10^3$ . It is not

clear how the strongly irradiated midplane would be able to maintain a constant temperature  $T_{\text{mid}}$  during this period of declining irradiation so as to lead to the kinematic viscosity coefficient  $\nu$  being constant with time in the outer disk. The constancy in  $\nu$  is needed in order to produce an exponential decay of the visual and X-ray fluxes in the model of King & Ritter (Mineshige et al. 1993).

4. In running long-term models with the parameters given in CCL so as to cover complete cycles of quiescence and outburst, we find that outbursts tend to be triggered frequently at small radii, confirming the analytical estimates of Lasota et al. (1996). Small outbursts occur every  $\sim 5$  years, whereas major outbursts that could be observed with typical all-sky monitors on X-ray satellites occur every  $\sim 50$  years. The rise times for the outbursts are  $\sim 10$  times longer than those commonly observed. When we include some evaporation of matter from the inner edge so as to produce a truncated  $\Sigma(r)$  profile in quiescence, we find that the smaller outbursts are eliminated and the rise times associated with the major outbursts are shortened but not enough to bring them into accord with observations. Therefore, we cannot confirm the conclusions of HLMN. The parameters for their system of interest, the microquasar GRO J1655–40, are sufficiently different from A0620–00 that a direct comparison of our respective findings may not be justified. In our modeling we find that, if a given model for the quiescence is not able on its own to prevent inside-out outbursts from occurring, then the addition of evaporation as an outside agent will not influence the  $\Sigma(r)$  profile to the extent required. We note that the form for  $\alpha$  arrived at by CCL is really only a constraint on  $\alpha$  in the hot state (i.e., on the upper, stable branch of the S-curve). Were one to artificially lower  $\alpha$  in quiescence by, for instance, reducing the proportionality constant,  $\alpha_0$ , it may be possible to force the matter to keep from evolving significantly at small radii and thereby prevent inside-out outbursts from triggering. Another possibility might be for the cooling front to “stall” at some radius  $\sim 10^9$ – $10^{10}$  cm so as to maintain a permanent hot, inner disk. This would deplete the  $\Sigma(r)$  profile for small radii and produce quiescent X-rays at a level commensurate with that seen in A0620–00 using a standard efficiency,  $\epsilon \sim 0.1$ .

For our standard model plus evaporation at a level  $\dot{M}_{\text{evap}} \sim 10^{14} \text{ g s}^{-1}$ , we produce outbursts with about the right spacing and amplitude as observed ( $t_{\text{recur}} \sim 50$ – $100$  years, outburst energy  $\delta E \simeq 3 \times 10^{44}$  ergs, accreted mass  $\delta M \simeq 5 \times 10^{24} \text{ g}$ , and peak absolute visual magnitude  $M_V \simeq +1$ ), although the rise times are too slow. As noted earlier, Lasota et al. (1996) point out that the standard model for the limit cycle instability in the BHXBs produces outbursts that recur too frequently because the inner disk radius is quite small, and they argue for evaporation to truncate the inner disk. If evaporation at a level  $\sim 10^{14} \text{ g s}^{-1}$  is correct, then the efficiency of accretion in the low state must be  $\epsilon \sim 10^{-4}$  (Narayan et al. 1996) to account for the observation of McClintock et al. (1995) of A0620–00 in quiescence. Following this one step further, since the efficiency in quiescence of the neutron star SXTs is still  $\epsilon \sim 0.1$ , there should exist a difference of  $\sim 10^3$  between the quiescent fluxes in BHXBs and neutron star binaries. This does not appear to be the case (Chen, Shrader, & Livio 1997; see their Fig. 14). Hence, while evaporation appears to be attractive in some ways, it may prove to be problematic in others.

5. The local values of the irradiation temperature are significantly less than the local values of the disk temperature in our standard model. King & Ritter (1998) argue quite the opposite, that irradiation is in fact strong during the outbursts of the BHXBs. They propose that the slow, exponential timescales for decay seen in A0620–00 and other similar systems are caused by the inability of the cooling front to form and shut off the flow of matter onto the BH. We may estimate the strength of the irradiation during outburst in A0620–00 in several ways. Warner (1987) found an empirical relation between absolute visual magnitude,  $M_V$ , and orbital period,  $P_{\text{orbital}}$ , for dwarf novae at maximum light in an outburst. A similar relation was found by van Paradijs & McClintock (1994; hereafter vPMc) for outbursts in BHXBs and neutron star binaries. Their relation was between  $M_V$  and  $(L_X/L_{\text{Edd}})^{1/2} P_{\text{orbital}}^{2/3}$ . The underlying cause for the Warner relation is thought to be the fact that the mass that can be stored up in quiescence in the limit cycle model is bounded from above by a critical value  $\int 2\pi r dr \Sigma_{\text{max}}$ , and this value scales with the size of the system (C93b; Warner 1995; Cannizzo 1998a). There seems to be general agreement that the triggering mechanism for outbursts in both classes of systems is the limit cycle instability, therefore the “maximum mass” concept should apply to both. By comparing the  $M_V$  values between the Warner and vPMc relations, one sees that the SXTs are intrinsically brighter than the dwarf novae. VPMc argue that the form of their relation implies a strong X-ray heating effect that leads to the bulk of the optical flux, through reprocessing, in the SXTs. In going between the dwarf novae and the neutron star SXTs, both of which presumably have  $\sim 1 M_{\odot}$  accretors, the comparison at a given orbital period should be direct and allow a pure estimate of the strength of the irradiation, since the sizes of the two systems and hence the surface areas of the accretion disks should be similar. For the BHXBs, however, one also needs to take into account the increased size of the disk, at a given orbital period, due to the presence of a more massive central object. If we compare the Warner and vPMc relations at the approximate orbital period of A0620–00, we see that  $\Delta M_V \sim 3$  mag. For  $P_{\text{orbital}}$  constant, the orbital separation scales as  $M_1^{1/3}$  (if  $M_1 \gg M_2$ ), so the radiating area of the disk that gives rise to the optical scales as  $M_1^{2/3}$ . In going from a  $\sim 0.7$ – $1 M_{\odot}$  white dwarf to a  $\sim 7 M_{\odot}$  BH, we increase the disk area and hence optical flux by  $\sim 7^{2/3}$ – $10^{2/3} \sim 4$ – $5$ , which reduces the difference,  $\Delta M_V$ , between the Warner and vPMc relations for an A0620–00 type system by  $\sim 2$  mag. Therefore,  $\Delta M_V(\text{corrected}) \sim 1$  mag. This comparison is admittedly crude because there may also exist a correction due to an effective temperature difference (J. van Paradijs 1997, private communication). We can obtain a more direct estimate simply by comparing our computed  $M_V$  for A0620–00 with that observed in the 1975 outburst. The shortfall in optical flux in the models that ignore irradiation must be due to the reprocessing of X-ray flux. Therefore, by determining the deficit, we learn how much of the optical flux comes from reprocessing and how much is due to viscous dissipation. This exercise has already been carried out by previous accretion disk limit cycle modelers specifically for A0620–00 using time-dependent models that did not include the effects of irradiation. HW modeled the *B*-band flux and determined  $\Delta M_B \sim 1$  mag at maximum light (see their Fig. 3), and MW modeled the *V*-band flux and found no difference between

their computed value and the observed value at maximum light (see their Fig. 10). In our model we find, for a face-on disk,  $M_V \sim +1$  at maximum light, whereas the observed value, corrected for extinction, is  $+0.7$  (vPMc). If we increase the inclination of our system to  $\sim 70^\circ$  (Haswell et al. 1993), our system becomes fainter, and we add  $\sim 1$  mag to our  $M_V(\text{peak})$  value, thereby giving  $\Delta M_V \sim 1$  between theory and observation, in line with the other estimates. Finally, in comparing our nonirradiated and irradiated models, we find at the peak of the outburst that  $T_{\text{irradiation}}/T_{\text{effective}} \sim 0.3$ – $0.4$  for  $n = 2$  thought to be applicable to the BHXBs. VPMc show that, for the temperature regime of relevance for the SXTs, the optical flux scales roughly as  $T_{\text{eff}}^2$ . Therefore, were we to self-consistently include the effects of irradiation in computing  $M_V$ , we would produce more optical flux by a factor of  $\sim 1.3^2$ – $1.4^2 \sim 2$ , which would subtract  $\sim 1$  mag from the inclination-corrected value  $M_V \simeq 2$ , bringing it back into accord with the observed value. In summary, it seems that the contribution of the reprocessed X-ray flux to the optical flux at peak light in A0620–00 is  $\sim 1$  mag, which means that its relative contribution is  $\sim 50\%$ – $70\%$ . This can be produced in the time-dependent disk models by a slight increase of the effective temperature in the inner part of the hot, viscous accretion disk. Were the entire disk to be strongly irradiated out to  $\sim 0.7$  of the Roche lobe of the primary so as to prevent the cooling wave from forming, as advocated by King & Ritter (1998), the optical flux would be overproduced with respect to what is observed in A0620–00.

We may quantify this last statement using the subroutine of our time-dependent code that calculates the *V*-band flux. If the entire disk is irradiated so that the cooling front is unable to form and propagate, that means the effective temperature must be at least  $\sim 9000$  K. The irradiation flux falls off as  $r^{-2}$ , so the radial distribution of the effective temperature, if it is dominated by irradiation flux, is  $r^{-1/2}$ . Inputting the law  $T_{\text{eff}}(r) = 9000 \text{ K } (r/r_{\text{outer}})^{-1/2}$ , where  $r_{\text{outer}} = 1.5 \times 10^{11} \text{ cm}$ , we find  $M_V = +0.45$ . For a moderate inclination, this becomes  $\sim 1.5$ . If the entire exponential decay observed in *V* during the 1975 outburst of A0620–00 were irradiation dominated, this is the faintest the disk could become. At the end of the exponential decay, however, one saw  $m_V \sim 14$ – $15$  (Lloyd et al. 1977), corresponding to an absolute *V* magnitude,  $M_V$ , of  $\sim 3$ – $4$  (vPMc)—fainter than seemingly allowed by the irradiation model. As a test of the zero point of the *V* calibration, we input  $T_{\text{eff}} = T_{\odot} = 5770 \text{ K}$  (constant with radius) and  $r_{\text{outer}} = R_{\odot} = 7 \times 10^{10} \text{ cm}$  and find  $M_V = +4.86$ . The accepted solar value is  $M_V = +4.83$  (Allen 1976). King & Ritter (1998) note the discrepancy between the X-ray to optical ratio in the computations of HW, and the observed value for A0620–00 in the 1975 outburst. The main problem is that HW’s calculated peak  $\dot{M}(r_{\text{inner}})$  value is  $\sim 3 \times 10^{19} \text{ g s}^{-1}$ —a factor  $\sim 30$  higher than observed. HW employed an early, experimental version of Cannizzo’s time-dependent disk code (from 1984), which may have led to numerical problems. For instance, they were forced to adopt an inner radius  $\sim 10$  times too large. In this paper we use a much more modern version of the code and find  $\dot{M} \sim 10^{18} \text{ g s}^{-1}$  as observed.

In this work we have chosen to concentrate on the most basic features of the BHXB outbursts: the recurrence time-

scale, the  $\sim 30$  day exponential decay, and the  $\lesssim 3$  day fast rise. We do not directly address the issue of the secondary maxima or reflares, which are frequently seen. Based on some of our findings, however, we may discuss previous work on the origin of the reflares. These are resurgences in the X-ray flux that are also seen to some extent in the optical, during which time the flux increases by a factor of  $\sim 2$  before resuming its decline. The decay properties after the reflare are much as before, so it is as if the light curve were displaced upward by a factor  $\sim 2$  beginning at a point  $\sim 60$ – $70$  days after the outburst starts. Several works have appeared concerning the reflares (Chen, Livio, & Gehrels 1993, hereafter CLG; Augusteijn, Kuulkers, & Shaham 1993; Mineshige 1994; K96; Kato, Mineshige, & Hirata 1995, hereafter KMH; IMK; Kuulkers, Howell, & van Paradijs 1996, hereafter KHvP; for a review see Wheeler 1996). One feature that some of the theories of the reflare share is that they involve irradiation, either of the secondary star so as to induce additional mass overflow that powers an increase in the luminosity by virtue of the extra material added to the disk (CLG; Augusteijn et al. 1993) or irradiation of the disk so as to reflect the cooling wave at one or two grid points as a heating front and momentarily rebrighthen part of the disk (K96).

In the context of the theories that rely on irradiation, it is interesting that the reflares seem to be uniquely associated with the BHXBs (Wheeler 1996). Reflars are not seen in the neutron star SXTs such as Cen X-4 and Aql X-1. According to our estimates of the strength of irradiation, and that of previous workers (HW; MW; van Paradijs 1996), however, irradiation is weak in the BHXBs. If reflars are unique to BHXBs, and if irradiation is weaker in BHXBs than in neutron star SXTs, it seems rather unlikely that irradiation can be the BHXB-specific parameter that causes reflars to occur only in the BHXBs. This makes it difficult to accept any of the irradiation-based models. Another consideration is that, whatever the physical mechanism is, it must be such that it leads to a delay time between onset of the main outburst and secondary reflare that scales with orbital period. The fact that the reflare in GRO J0422+32 occurred  $\sim 45$  days after primary maximum, whereas in A0620–00 it occurred  $\sim 55$  days after primary maximum, led CLG to predict an orbital period less than 7 hours for this system. The period was later found to be 5.1 hr (Chevalier & Ilovaisky 1994; Orosz & Bailyn 1995).

What unique property of BHXBs—something that would not be true for the neutron star SXTs—exists that could account for the reflars? This has already been answered by many authors: it is the extreme value of the mass ratio  $q = M_2/M_1$  (Bailyn 1992; KMH; IMK; KHvP). This ratio is much smaller for BHXBs than for neutron star SXTs, and this can lead to resonances occurring within  $\sim 0.7$  of the Roche lobe of the primary wherein the disk is constrained by tidal truncation to exist. One observes superhumps (SHs) during superoutbursts (SOs) in the SU UMa class of dwarf novae (Warner 1995). The SHs are thought to be caused by the fact that the 3:1 commensurability resonance with the binary orbital period lies within the accretion disk for  $q \lesssim 0.25$  (Whitehurst 1988, 1994, 1995), but lies beyond the point of tidal truncation for  $q \gtrsim 0.25$ . In fact, SHs are only seen in short orbital period dwarf novae for which  $q \lesssim 0.25$ . Whitehurst showed that when the condition  $q \lesssim 0.25$  is fulfilled, the outer disk acquires an elliptical shape that precesses in the corotating frame of the binary, and this

precession causes the distance through which the mass stream must fall before striking the outer disk to vary, thereby modulating the light curve on a timescale equal to the orbital period plus a few percent. Osaki (1989) combined the disk instability model with a proposed “tidal instability,” which he envisioned to occur whenever Whitehurst’s condition for superhumps becomes satisfied. Osaki’s thermal-tidal (TT) instability allows for superoutbursts in the SU UMa stars by imagining that, whenever the outer edge of the disk expands beyond the 3:1 resonance in the disk, the increased tidal torque on the disk enforces a contraction of  $r_{\text{outer}}$  by  $\sim 10\%$ – $20\%$ . The mass that was present in the disk at the start of the outburst is confined to a smaller volume, and the increase in  $\Sigma(r_{\text{outer}})$  relative to  $\Sigma_{\text{min}}(r_{\text{outer}})$  produces an “overfilled” disk that prevents the cooling wave from starting until a sizable fraction of the disk matter has accreted onto the central object. The motivation for the contraction of the outer disk was not obvious, based on Whitehurst’s time-dependent calculations, and led to criticisms (Whitehurst 1994; Cannizzo 1996a). Recent work by Murray (1998), which utilizes a more advanced smoothed particle hydrodynamics model than was available to Whitehurst, however, does in fact show a contraction of the outer radius that is coincident with the growth into the nonlinear regime of the elliptical disk induced by the 3:1 resonance. This gives credence to Osaki’s model.

What does this have to do with the reflars in the BHXB outburst light curves? A potentially key observation is that, in the BHXB GRO J0422+32, SHs appeared in the outburst at about the same time as the reflare, thereby arguing for a direct connection between the nonlinear outcome of the 3:1 instability—namely the formation of an eccentric disk and concomitant SHs—and the reflare (KMH, KHvP). The crucial difference that the global effect the disk contraction has in going from accretion disks in dwarf novae to those in the BHXBs has to do with the growth time to reach the nonlinear regime of the tidal instability. Several workers have suggested a direct connection between the SHs and the reflars (KMH, IMK, KHvP), namely, that it is the contraction of the disk in Osaki’s TT model that leads to the reflars. IMK argue that the 3:1 resonance growth time varies as  $t_{\text{grow}} \sim 1/[\Omega(r_{\text{outer}})]$ , where  $\Omega(r_{\text{outer}})$  is the Keplerian frequency at the outer disk edge. They point out that  $t_{\text{grow}}$  is about 30 times larger for the BHXBs than for the SU UMa stars. For normal outbursts that turn into SOs in the SU UMa stars by virtue of the expansion of  $r_{\text{outer}}$  beyond the 3:1 resonance radius, the time,  $t_{\text{grow}}(\text{SU UMa})$ , is  $\sim 1$ – $3$  days, so that one sees in the light curves first a rise to maximum associated with the normal outburst, then a brief dip, and then a rebrightening to maximum as the forced contraction of the accretion disk becomes active and the disk gas gets confined to a smaller radius. This constitutes the formal start of the SO, marked subsequently by a long-term slower-than-exponential decline that typifies decays from maximum light in which the cooling front is unable to propagate. If  $t_{\text{grow}} \sim 100$  days for the BHXBs, this would have important consequences for the interaction of the contraction phase with the inward propagation of the cooling front. This timescale is about three  $e$ -foldings for the time to deplete the mass of the hot part of the accretion disk, or one  $e$ -folding time  $|d \ln r_F / dt|^{-1}$  for the cooling front to move inward (CCL), so the cooling front has already had ample time to travel inward a considerable distance from  $r_{\text{outer}}$  as defined by the tidal truncation and subsequently redefined

by the increased degree of tidal truncation due to the 3:1 resonance-induced elliptical disk. There is no opportunity for the cooling front to be prevented from forming as in the SU UMa SOs, and yet the gas in the accretion disk must be confined in some manner to a smaller value. It is difficult to estimate the degree of this contraction without doing a detailed calculation, especially considering the fact that the contraction occurs primarily in the outer, cold portion of the disk. One suspects that the brief period of augmentation in the local  $\Sigma(r)$  values would produce a reflection of the cooling wave as a heating wave, which would propagate out some distance and then reflect inward again as a cooling front. This is found in time-dependent calculations (IMK). The amplitude of the reflares observed in the BHXB outburst light curves are about a factor of 2 with respect to the X-ray flux observed just prior to the start of the reflare. This would not require a large reflection in order to be produced. The reflares caused by the reflection of cooling waves into heating waves seen in some of the light curves in CCL showed increases of  $\sim 10$  in flux. (Their cause is thought to be numerical, however, and not physical.) In summary, the fast growth time for the 3:1 instability in the SU UMa stars leads to an immediate contraction in  $r_{\text{outer}}$  and to a consequent overfilled disk that can only decay viscously (since the cooling front cannot propagate), whereas the slow growth time for the 3:1 instability in the BHXBs means that the contraction, when it does occur, is too late to produce an overfilled disk. Instead, one has only a minor readjustment in  $\Sigma(r)$  that produces a reflected transition front and resultant reflare.

IMK attempted to calculate models using the TT instability for BHXBs, but various deficiencies in their work led to outbursts that did not resemble those observed. They use a low-resolution logarithmic spacing,  $N \sim 20\text{--}40$ , to cover a dynamic range in disk radii,  $r_{\text{outer}}/r_{\text{inner}} > 10^4$ , they use a parametrization of  $\alpha \propto r^{0.3}$  (C94), which was criticized as not being valid for BHXB parameters (CCL), and their model contains detailed ad hoc prescriptions for the functional form of the increase in the tidal torque associated with the TT instability (both  $\alpha$  and the torque proportionality constant each have about six adjustable parameters). The light curve they present covering an outburst with the TT induced reflare shows a factor of  $\sim 10^3$  increase in  $L_X$  in the reflare, rather than the observed factor  $\sim 2$  increase. The decay characteristics are also not as observed. Nevertheless, their model represents a first step toward a complete theory of outburst plus reflare in a time-dependent model. Work is currently underway to activate and test the portion of our code that allows for a variable outer disk radius so as to test the global manifestation of Osaki's TT instability in the BHXBs.

#### 4. CONCLUSION

We have investigated several aspects of the accretion disk limit cycle mechanism as it applies to BHXBs. Our main impetus is to extend work reported in CCL by running more extensive time-dependent models, to cover complete cycles of outburst and quiescence, and to look in detail at several aspects of the model not studied by CCL. We find that the explanation for the cooling front speed put forth by VW seems to account for the deviation from steady state flow that we observe. In running complete cycles, we find a strong tendency, using the CCL  $\alpha$  form, for frequent out-

bursts to occur that begin at small radii in the disk and have slow rise times, in contrast to the observations. Evaporation of material from the inner disk does not shift the surface density distribution enough to decrease the rise times sufficiently, although it does increase the recurrence times for outbursts to an acceptable value (Lasota et al. 1996). A separate issue is the necessity of having some mechanism distinct from the standard limit cycle operating in order to supply material to accrete onto the central object in quiescence so as to provide substantial X-ray and EUV radiation. Finally, for our standard model, which is meant to represent a system like A0620–00, irradiation of the disk does not appear to be strong enough to change the structure significantly. This may pose a challenge for workers that seek to invoke irradiation to prevent the cooling front from propagating. Also, the apparent weakness of irradiation in the BHXBs relative to the neutron star binaries may present problems for theories of the reflare that are based on irradiation.

This paper is not intended to be the final word on this subject but should serve only to pose additional questions that must be looked into. There is clearly much more work to be done. In spite of our efforts, we have failed to produce a successful standard model for A0620–00 that reproduces not only the  $\sim 30$  day  $e$ -folding time exponential decay and  $\sim 60$  year recurrence timescale for outbursts but also the fast rise, which is  $\sim 3\text{--}5$  days. We have purposely avoided introducing modifications to the  $\alpha$  form utilized by CCL in order to provide continuity with that work. It now appears, however, that it may prove necessary to reduce  $\alpha$  in the low state below that which would naturally occur using the CCL scaling. This could be carried out, for instance, by reducing  $\alpha_0$ . There may be other ways to get the fast rise, such as having a stalled cooling front that would deplete  $\Sigma(r)$  for small  $r$ .

In this work, we have only activated the portion of our code that calculates the irradiation temperature based on the central flux from the disk and the local shape, as explained in Tuchman et al. (1990). The next step is to activate and test the portion that also “corrects” the local disk temperature (both effective and midplane) based on the irradiation temperature, which would in turn affect the global evolution of the disk (as in K96). Since the irradiation temperature does not even approach the effective temperature for parameters relevant to A0620–00, the kinematic effect on the disk would be insignificant. For the neutron star systems, however, irradiation will most likely play an important role.

We have also chosen not to activate the part of the code that treats the variation of outer disk radius (Smak 1984). This may affect the nature of the light curves accompanying the outbursts, in particular the rise times, by virtue of the mass swept up at large radii by the arrival of low angular momentum material from the secondary star.

We acknowledge useful discussions with W. Chen, J.-M. Hameury, A. King, E. Kuulkers, J.-P. Lasota, C. Mauche, J. McClintock, R. Narayan, J. van Paradijs, E. Vishniac, B. Warner, and C. Wheeler. J. K. C. was supported through the long-term scientist program under the Universities Space Research Association (USRA contract NAS 5-32484) in the Laboratory for High Energy Astrophysics at Goddard Space Flight Center.

## REFERENCES

- Allen, C. W. 1976, *Astrophysical Quantities* (London: Athlone), 162
- Angelini, L., & Verbunt, F. 1989, *MNRAS*, 238, 697
- Augusteijn, T., Kuulkers, E., & Shaham, J. 1993, *A&A*, 279, L13
- Bailyn, C. D. 1992, *ApJ*, 391, 298
- Bailyn, C. D., Jain, R. K., Coppi, P., & Orosz, J. A. 1996, *BAAS*, 28, 1329
- Bailyn, C. D., Orosz, J. A., McClintock, J. E., & Remillard, R. A. 1995, *Nature*, 378, 157
- Cannizzo, J. K. 1993a, in *Accretion Disks in Compact Stellar Systems*, ed. J. C. Wheeler (Singapore: World Scientific), 6
- . 1993b, *ApJ*, 419, 318 (C93b)
- . 1994, *ApJ*, 435, 389 (C94)
- . 1996a, *Mem. Soc. Astron. Italiana*, 67, 227
- . 1996b, *Mem. Soc. Astron. Italiana*, 67, 269
- . 1996c, *ApJ*, 473, L41
- . 1998a, *ApJ*, 493, 426
- . 1998b, in *ASP Conf. Ser., The 13th North American Workshop on Cataclysmic Variables*, ed. S. B. Howell, E. Kuulkers, & C. Woodward (San Francisco: ASP), in press
- Cannizzo, J. K. 1998c, in preparation
- Cannizzo, J. K., Chen, W., & Livio, M. 1995, *ApJ*, 454, 880 (CCL)
- Cannizzo, J. K., Lee, H. M., & Goodman, J. 1990, *ApJ*, 351, 38
- Cannizzo, J. K., & Wheeler, J. C. 1984, *ApJS*, 55, 367
- Cannizzo, J. K., Wheeler, J. C., & Ghosh, P. 1982, in *Pulsations in Classical and Cataclysmic Variable Stars*, ed. J. P. Cox & C. J. Hansen (Boulder: Univ. of Colorado Press), 13
- . 1985, in *Proc. Cambridge Workshop on Cataclysmic Variables and Low-Mass X-Ray Binaries*, ed. D. Q. Lamb & J. Patterson (Dordrecht: Reidel), 307
- Cannizzo, J. K., Wheeler, J. C., & Polidan, R. S. 1986, *ApJ*, 301, 634 (CWP)
- Chakrabarti, S. 1996a, *Phys. Rep.*, 266, 229
- . 1996b, *ApJ*, 464, 664
- Chen, W., Livio, M., & Gehrels, N. 1993, *ApJ*, 408, L5 (CLG)
- Chen, W., Shrader, C. R., & Livio, M. 1997, *ApJ*, 491, 312
- Chevalier, C., & Ilovaisky, S. A. 1994, *IAU Circ.* 6118
- Elvis, M., Page, C. G., Pounds, K. A., Ricketts, M. J., & Turner, M. J. L. 1975, *Nature*, 257, 291
- Esin, A. A., McClintock, J. E., & Narayan, R. 1997, *ApJ*, 489, 865
- Hameury, J.-M., Lasota, J.-P., McClintock, J. E., & Narayan, R. 1997, *ApJ*, 489, 234 (HLMN)
- Haswell, C., Robinson, E. L., Horne, K., Stiening, R. F., & Abbott, T. M. C. 1993, *ApJ*, 411, 801
- Huang, M., & Wheeler, J. C. 1989, *ApJ*, 343, 229 (HW)
- Hynes, R. I., Haswell, C. A., Chen, W., & Shrader, C. R. 1996, *BAAS*, 28, 1314
- Ichikawa, S., Mineshige, S., & Kato, T. 1994, *ApJ*, 435, 748 (IMK)
- Ichikawa, S., & Osaki, Y. 1992, *PASJ*, 44, 15
- . 1994, in *Theory of Accretion Disks—2*, ed. W. Duschl (Dordrecht: Kluwer), 169
- Kato, T., Mineshige, S., & Hirata, R. 1995, *PASJ*, 47, 31 (KMH)
- Kim, S.-W., Wheeler, J. C., & Mineshige, S. 1994, in *The Evolution of X-ray Binaries*, ed. S. S. Holt & C. S. Day (AIP: New York), 213 (K94)
- . 1996, in *IAU Colloq. 158, Cataclysmic Variables and Related Objects*, ed. A. Nye & J. H. Wood (Dordrecht: Kluwer), 139 (K96)
- King, A. R., & Ritter, H. 1998, *MNRAS*, in press
- Kuulkers, E., Howell, S. B., & van Paradijs, J. 1996, *ApJ*, 462, L87 (KHvP)
- Lasota, J.-P. 1996a, in *IAU Symp. 165, Compact Stars in Binaries*, ed. J. van Paradijs, E. P. J. van den Heuvel, & E. Kuulkers (Dordrecht: Kluwer), 43
- Lasota, J.-P. 1996b, in *IAU Colloq. 158, Cataclysmic Variables and Related Objects*, ed. A. Nye & J. H. Wood (Dordrecht: Kluwer), 385
- Lasota, J.-P., Narayan, R., & Yi, I. 1996, *A&A*, 314, 813
- Lin, D. N. C., Papaloizou, J., & Faulkner, J. 1985, *MNRAS*, 212, 105
- Lin, D. N. C., & Taam, R. E. 1984, in *High Energy Transients in Astrophysics*, ed. S. E. Woosley (Santa Cruz: AIP), 83
- Liu, F. K., Meyer, F., & Meyer-Hofmeister, E. 1995, *A&A*, 300, 823
- Lloyd, C., Noble, R., & Penston, M. V. 1977, *MNRAS*, 179, 675
- Lubow, S. H., & Shu, F. H. 1975, *ApJ*, 198, 383
- Ludwig, K., & Meyer, F. 1998, *A&A*, 329, 559
- Mauche, C. W. 1996, *IAU Colloq. 152, Astrophysics in the Extreme Ultraviolet*, ed. S. Bowyer & R. F. Malina (Dordrecht: Kluwer), 317
- McClintock, J. E., Horne, K., & Remillard, R. A. 1995, *ApJ*, 442, 358
- McClintock, J. E., Petro, L. D., Remillard, R. A., & Ricker, G. R. 1983, *ApJ*, 266, L27
- Meyer, F. 1984, *A&A*, 131, 303
- . 1990, in *Reviews in Modern Astronomy 3: Accretion and Winds*, ed. G. Klare (Berlin: Springer), 1
- Meyer, F., & Meyer-Hofmeister, E. 1981, *A&A*, 104, L10
- . 1983, *A&A*, 128, 420
- . 1984, *A&A*, 132, 143
- . 1994, *A&A*, 288, 175
- Mineshige, S. 1994, *ApJ*, 431, L99
- Mineshige, S., & Wheeler, J. C. 1989, *ApJ*, 343, 241 (MW)
- Mineshige, S., Yamasaki, T., & Ishizaka, C. 1993, *PASJ*, 45, 707
- Murray, J. R. 1998, *MNRAS*, in press
- Narayan, R., McClintock, J., & Yi, I. 1996, *ApJ*, 457, 821
- Orosz, J. A., & Bailyn, C. D. 1995, *ApJ*, 446, L59
- Osaki, Y. 1989, *PASJ*, 41, 1005
- . 1996, *PASP*, 108, 39
- Pringle, J. E., Verbunt, F., & Wade, R. A. 1986, *MNRAS*, 221, 169
- Shakura, N. I., & Sunyaev, R. A. 1973, *A&A*, 24, 337
- Smak, J. 1983, *ApJ*, 272, 234
- . 1984, *Acta Astron.*, 34, 161
- Tanaka, Y., & Shibazaki, N. 1996, *ARA&A*, 34, 607
- Tuchman, Y., Mineshige, S., & Wheeler, J. C. 1990, *ApJ*, 359, 164
- van Paradijs, J. 1996, *ApJ*, 464, L139
- van Paradijs, J., & McClintock, J. E. 1994, *A&A*, 290, 133 (vPMc)
- . 1995, in *X-ray Binaries*, ed. W. H. G. Lewin, J. van Paradijs, & E. P. J. van den Heuvel (Cambridge: Cambridge Univ. Press), 58
- van Paradijs, J., & Verbunt, F. 1984, in *High Energy Transients in Astrophysics*, ed. S. E. Woosley (Santa Cruz: AIP), 49
- Vishniac, E. T. 1997, *ApJ*, 482, 414
- Vishniac, E. T., & Wheeler, J. C. 1996, *ApJ*, 471, 921
- Warner, B. 1987, *MNRAS*, 227, 23
- . 1995, *Cataclysmic Variable Stars* (Cambridge: Cambridge Univ. Press)
- Wheeler, J. C. 1996, in *Relativistic Astrophysics*, ed. B. Jones & D. Markovic (Cambridge: Cambridge Univ. Press), in press
- Whitehurst, R. 1988, *MNRAS*, 232, 35
- . 1994, *MNRAS*, 266, 35
- . 1995, *MNRAS*, 277, 655
- Zhang, S. N., Cui, W., & Chen, W. 1997, *ApJ*, 482, L155